Just the once will not hurt: DNA suggests species lumping over two oceans in deep-sea snails (*Cryptogemma*)

PAUL ZAHARIAS[1]*,[®], YURI I. KANTOR[2], ALEXANDER E. FEDOSOV[2], FRANCESCO CRISCIONE[3],[®], ANDERS HALLAN[3], YASUNORI KANO[4], JÉRÉMIE BARDIN[5] and NICOLAS PUILLANDRE[1]

[1]*Institut Systématique Evolution Biodiversité (ISYEB), Muséum National d'Histoire Naturelle, CNRS, Sorbonne Université, EPHE, Université des Antilles, 43 rue Cuvier, CP 26, 75005 Paris, France*
[2]*A. N. Severtsov Institute of Ecology and Evolution, Russian Academy of Sciences, Leninski prospect 33, 119071 Moscow, Russian Federation*
[3]*Australian Museum Research Institute, Australian Museum, Sydney, NSW 2010, Australia*
[4]*Atmosphere and Ocean Research Institute, The University of Tokyo, 5-1-5 Kashiwanoha, Kashiwa, Chiba 277-8564, Japan*
[5]*Centre de Recherche en Paléontologie – Paris (CR2P-UMR 7207), Sorbonne Université-CNRS-MNHN, Site Pierre et Marie Curie, 4 place Jussieu, Paris Cedex 05, France*

The practice of species delimitation using molecular data commonly leads to the revealing of species complexes and an increase in the number of delimited species. In a few instances, however, DNA-based taxonomy has led to lumping together of previously described species. Here, we delimit species in the genus *Cryptogemma* (Gastropoda: Conoidea: Turridae), a group of deep-sea snails with a wide geographical distribution, primarily by using the mitochondrial *COI* gene. Three approaches of species delimitation (ABGD, mPTP and GMYC) were applied to define species partitions. All approaches resulted in eight species. According to previous taxonomic studies and shell morphology, 23 available names potentially apply to the eight *Cryptogemma* species that were recognized herein. Shell morphometrics, radular characters and geographical and bathymetric distributions were used to link type specimens to these delimited species. In all, 23 of these available names are here attributed to seven species, resulting in 16 synonymizations, and one species is described as new: ***Cryptogemma powelli*** **sp. nov.** We discuss the possible reasons underlying the apparent overdescription of species within *Cryptogemma*, which is shown here to constitute a rare case of DNA-based species lumping in the hyper-diversified superfamily Conoidea.

ADDITIONAL KEYWORDS: species delimitation – species description – ABGD – GMYC – PTP – deep-sea species – larval dispersal – cosmopolitan species.

INTRODUCTION

The advent of integrative taxonomy (Dayrat, 2005; Will *et al.*, 2005), mainly driven by the molecular revolution, has led to a remodelling of the practice of species delimitation, extending the use of standardized approaches in the field of taxonomy (e.g. Lefébure *et al.*, 2006). Several of the resulting studies, often based primarily on molecular data, have revealed numerous species complexes, thus increasing the number of delimited species, commonly referred to as 'cryptic species', within such groups (Bickford *et al.*, 2007; Fišer *et al.*, 2018). The difficulty in assigning names and/or describing these newly delimited species can constitute an impediment, especially for non-taxonomists.

Indeed, when new species are discovered, nearly half of them remain undescribed, at least not described in the publication where they are revealed (Pante *et al.*, 2015). Thus, the splitting effect of integrative taxonomy is not accompanied by adequate taxonomic effort, resulting in many undescribed species. This lack of an appropriate taxonomic procedure may have consequences in various fields, such as ecology and conservation (e.g. Iglésias *et al.*, 2010).

Conversely, there have been instances when integrative taxonomy, by incorporating molecular data, has led to the lumping of taxa that were originally described using morphological and anatomical characters only (e.g. Dejaco *et al.*, 2016; Chan *et al.*, 2018). Such instances may occur when, contrary to the occurrence of cryptic species, intraspecific morphological variability is equal to or greater than interspecific variability (e.g. Puillandre *et al.*, 2010). These phenomena may have biological causes (e.g. sexual dimorphism, allometry during ontogeny, phenotypic plasticity) or may simply be artefacts of a particular taxonomic practice (some taxonomists tend to split more than others). Unfortunately, these cases are difficult to investigate for taxa where morphological characterization is not formalized, genomic resources are poor and/or known specimens are rare and deposited in different institutions. Nevertheless, the investigation of whether or not different forms correspond to different species should rely on a combination of modern species delimitation approaches and solid taxonomic expertise in order to clarify both the boundaries and the taxonomic status of a given taxon.

The Conoidea (Neogastropoda) is an extremely diversified lineage of marine gastropods, traditionally divided into Terebridae, Conidae and Turridae (Bouchet *et al.*, 2011). Recent molecular phylogenies have significantly redefined boundaries within the superfamily (Puillandre *et al.*, 2011; Abdelkrim *et al.*, 2018a), leading to a redefinition of the turrids. The family Turridae H. Adams & A. Adams, 1853 (1838) is now a monophyletic group that encompasses a few morphologically well-defined monophyletic genera, such as *Gemmuloborsonia* Shuto, 1989, *Polystira* Woodring, 1928, *Lophiotoma* T. L. Casey, 1904 and the '*Xenuroturris* Iredale, 1929/*Iotyrris* Medinskaya & Sysoev, 2001 complex', that have been revised in recent years (Puillandre *et al*, 2010, 2017; Todd & Rawlings, 2014; Abdelkrim *et al.*, 2018b). In some cases, the integrative taxonomy approach has uncovered cryptic species that have been described in the same studies in which they were revealed. However, a considerable proportion of turrid species have been left in the paraphyletic genus *Gemmula*, for which it was estimated that fewer than half the number of species have been described so far (Puillandre *et al.*, 2012). Puillandre *et al.* (2012) also called for

the complete revision of *Gemmula* and suggested that the high number of species and the suspected global morphological stasis of the group are likely to explain why this group has remained unrevised until now. Moreover, revising the *Gemmula* group would be tantamount to revising the entire Turridae, given that independent '*Gemmula*-like' lineages are distributed all over the turrid tree (Puillandre *et al.*, 2012). Finally, although a high number of undescribed species was estimated in *Gemmula*, it is not clear whether all the independent '*Gemmula*-like' lineages include undescribed species or whether some lineages will require splitting of previously described species, whereas others will imply lumping of previously described species, or a combination of both splitting and lumping. Hence, we propose that the taxonomic revision should be partitioned by focusing on smaller monophyletic groups that can be revised one by one, in order to resolve progressively the taxonomic predicament of *Gemmula* as it stands at present.

The first group we identified is a clade of deep-water species, hereafter named '*Cryptogemma*', that has already been used as a case study to illustrate congruent species hypotheses in the integrative taxonomy framework designed by Puillandre *et al.* (2012: fig. 5), comprising five species of Turridae attributed to three genera. We completed the dataset from Puillandre *et al.* (2012) with recent field sampling and material from museums and applied an integrative taxonomy approach primarily based on the analysis of the barcode fragment of *COI* with additional data on the geography and bathymetry included a posteriori to help with attribution of existing names to the molecular species hypotheses. Furthermore, we significantly improved the resolution of morphological studies by carrying out a formalized analysis of the morphology of the teleoconch and protoconch and by examining radulae in all sequenced species. The sequencing of a few type specimens and the formalized morphological analysis allow us to attribute type specimens confidently to molecular species. Our results enable a comprehensive revision of *Cryptogemma*. Instead of finding the usual splitting effect of molecular-based integrative taxonomy, our study led to an unexpected number of new synonymies and the description of only one new species.

ABBREVIATIONS

Museums and repositories: AMS, Australian Museum, Sydney, NSW, Australia; AWMM, Auckland War Memorial Museum, Auckland, New Zealand; BPBM, Bernice Pauahi Bishop Museum, Honolulu, HI, USA; FMNH, Field Museum of Natural History, Chicago, IL, USA; MNHN, Muséum national d'Histoire naturelle, Paris, France; NHMUK, Natural History Museum,

London, UK; USNM, National Museum of Natural History, Smithsonian Institution, Washington, DC, USA; ZMB, Museum für Naturkunde, Humboldt-Universität, Berlin, Germany; ZMMU, Zoological Museum of Moscow University, Moscow, Russian Federation; ZSIC, Zoological Survey of India, Calcutta, India.

Others: AL, shell aperture length; OD, original designation of type species of a genus PD, protoconch diameter; PL, protoconch length; R/V, research vessel; st., station.

MATERIAL AND METHODS

The integrative taxonomy pipeline followed in this study comprises three main steps. First, most samples were sequenced at least for the cytochrome *c* oxidase subunit I (*COI*) gene fragment, without necessarily receiving a preliminary morphological identification to the species level. Second, automated species delimitation methods were used to delimit molecular operational taxonomic units (MOTUs), resulting in primary species hypotheses. Third, MOTUs were assessed using alternative gene fragments, morphology, geography and bathymetry, resulting in the final species hypotheses.

SAMPLING

As a part of our background activity, most neogastropods collected during field expeditions organized by the Muséum national d'Histoire naturelle (MNHN) are processed for DNA extraction and sequencing of the barcode fragment of the *COI* gene. Among the processed material, all specimens for which the barcode sequences clustered into the *Cryptogemma* clade were included in this study. These samples were collected during the following field expeditions in the Indo-Pacific and West Atlantic: EBISCO and KANADEEP in the Chesterfield Islands; CONCALIS, EXBODI, KANACONO, TERRASSES and NORFOLK 2 in New Caledonia; MIRIKY and ATIMO VATAE in Madagascar; MAINBAZA in Mozambique, BIOMAGLO in Mayotte; BIOPAPUA, KAVIENG, MADEEP and PAPUA NIUGINI in Papua New Guinea; AURORA 2007 and PANGLAO 2004 in the Philippines; SALOMON 2 and SALOMONBOA 3 in the Solomon Islands; TARASOC in the Society-Tuamotu Islands; TAIWAN 2013, NANHAI 2014, DONGSHA 2014 and ZHONGSHA 2015 in Taiwan; and GUYANE 2014 in French Guiana (expeditions.mnhn.fr). Additional samples were collected during Japanese expeditions: T/V 'Nagasaki-maru' cruise N275 and R/V 'Tansei-maru' cruise KT-12-32 in Japan. We completed this sampling with specimens from the Australian Museum (AMS), Zoological Museum of Moscow State University (ZMMU) and the National Museum of Natural History (USNM) that could potentially belong to this clade, based on their morphology and the available corresponding sequences in GenBank. Twelve specimens from AMS were collected during the IN2017_V03 – Sampling the Abyss cruse (2017). A paratype of *Ptychosyrinx lordhoweensis* Kantor & Sysoev, 1991 (R/V 'Dmitry Mendeleev', 16th cruise, st. 1245, no. Lc14353; Kantor & Sysoev, 1991) from the ZMMU was used for DNA extraction. Samples from USNM were also selected for molecular analyses: three paralectotypes of *Gemmula benthima* Dall, 1908 (USS *Albatross*, st. 2807, 3360, 3365; USNM numbers 96485, 123087 and 123092; Kabat, 1996) and one specimen of *Ptychosyrinx carynae* (Haas, 1949), USNM 832922. For USNM samples, *G. benthima* specimens were preserved dry, whereas the *P. carynae* specimen was probably fixed in formalin before conservation in ethanol.

The MNHN specimens processed before 2012 and all AMS specimens chosen for molecular analysis were anaesthetized using an isotonic solution of $MgCl_2$ before fixation in 96% ethanol. The MNHN specimens processed after 2012 were microwaved and fixed in 96% ethanol (Galindo *et al.*, 2014). In some cases, shells were subsequently drilled to extract the retracted animals. Japanese specimens were boiled in water at 70–90 °C for 0.1–0.5 min before preservation in 99% ethanol. The ZMMU specimens were probably fixed and preserved in 75–80% ethanol.

DNA SEQUENCING

DNA from MNHN samples was extracted using the Epmotion 5075 robot (Eppendorf), following the manufacturer's recommendations. DNA from AMS samples was extracted from small pieces of foot muscle by use of a Bioline Isolate II Genomic DNA extraction kit for animal tissue, following the standard procedure of the manual. DNA from ZMMU and USNM samples was extracted using the EZNA Mollusc DNA Kit (Omega Bio-Tek Inc.), following the manufacturer's recommendations. For most samples, the barcode fragment (658 bp) of the mitochondrial *COI* gene was amplified using the universal primers LCO1490/HCO2198 (Folmer *et al.*, 1994). Polymerase chain reactions (PCRs) were performed using a previously well-established protocol (Puillandre *et al.*, 2017). For the ZMMU and USNM samples, the barcode fragment was amplified in two fragments, one with the LCO1490 and a newly designed primer (conoCOIintR: GCNCATGCHGGNGGNTCWGTW) and the other with another newly designed primer (conoCOIintF: TCWTCAGCTGCNGTWGAAAGNGG) and the HCO2198 primer. Both fragments overlap for ~50 nucleotides. The PCR mix was the same as for LCO1490/HCO2198, except that bovine serum albumin

(10 mg/mL) was used instead of dimethyl sulfoxide. The amplification procedure was also similar, except that the annealing temperature was 47 °C, with 40 cycles instead of 35.

A fragment of the mitochondrial 12S rRNA gene was amplified using the universal primers 12S1/12S3 (Simon *et al.*, 1991) and PCRs were performed using a previously established protocol (Puillandre *et al.*, 2011). The PCR products were purified and sequenced by the Eurofins sequencing facility. The 28S primers used at AMS were second option (Dayrat *et al.*, 2001; Jovelin & Justine, 2001). Amplification of 28S consisted of an initial denaturation step at 94 °C for 4 min, followed by 30 cycles of denaturation at 94 °C for 30 s, with annealing set to 57 °C for 45 s, followed by extension at 72 °C for 1 min. The final extension was at 72 °C for 5 min.

SPECIES DELIMITATION

The *COI* sequences were aligned manually using MEGA X (Kumar *et al.*, 2018); 12S and 28S sequences were aligned using MUSCLE (Edgar, 2004) as implemented in MEGA X and checked by eye. Phylogenetic reconstruction methods were applied to the *COI* alignment, plus a concatenation of the *COI*, 12S and 28S alignments with one specimen per species (see Results section).

Automatic Barcode Gap Discovery (ABGD), Generalized Mixed Yule Coalescent (GMYC) and multi-rate Poisson tree processes (mPTP) methods were applied to the *COI* dataset. All three methods are exploratory and aim at finding clusters of specimens corresponding to species, but they differ strongly in several aspects. The ABGD method is based on genetic distances only and automatically detects the gap (the so-called 'barcode gap') between intra- and interspecific distances, which is then used to delimit species hypotheses. In contrast, GMYC and mPTP rely on phylogenetic trees. The GMYC method uses an ultrametric tree and looks for a transition between speciation and coalescent nodes. The mPTP method also delimits species by identifying the transition between the inter- and intraspecific parts of the tree, but requires only a phylogeny with the branch length being proportional to the number of substitutions and relies on the mutation rate instead of the branching rate.

For ABGD, the Web version (http://wwwabi.snv.jussieu.fr/public/abgd/) and the default parameters were used, with a Kimura (K80) TS/TV model implemented. Maximum likelihood (ML) trees were constructed for *COI* and the concatenated (*COI* + 12S + 28S) alignments using IQ-TREE v.1.6.3 (Nguyen *et al.*, 2015), with 100 bootstraps. For all alignments, *COI* was consistently divided into three partitions, corresponding to the three codon positions, and 12S and 28S each considered as a single partition. The best model for each partition was evaluated using ModelFinder as implemented in IQ-TREE (Kalyaanamoorthy *et al.*, 2017).

The mPTP approach of species delimitation (Kapli *et al.*, 2017) was performed on the *COI* maximum likelihood tree, using both ML delimitation with default parameters and Markov chain Monte Carlo method, with a Markov chain of 200 000 000 generations, a sampling frequency of 2000 generations and a burn-in set at 25%. Bayesian trees were reconstructed using BEAST v.2.5.0 (Bouckaert *et al.*, 2019), running 200 000 000 generations on the *COI* dataset, with a sampling frequency every 4000 generations and a burn-in set at 10%. The *COI* dataset was partitioned by codon position for model evaluation, and prior values were set as in the study by Puillandre *et al.* (2017). The resulting trees were combined using TreeAnnotator as implemented in BEAST2, with node heights corresponding to the mean heights of all trees. The 'single threshold' method of GMYC was applied using the resulting tree. Finally, a non-ultrametric Bayesian tree was reconstructed for the *COI* and concatenated datasets using MrBayes v.3.2.6 (Ronquist & Huelsenbeck, 2003), with each of the two runs consisting of eight Markov chains and 20 000 000 generations and a sampling frequency of 2000. The analysis was performed on the Cipres Science Gateway (http://www.phylo.org/portal2). The consensus tree was calculated with the burn-in set at 20%.

Four species of Turridae were used as outgroups: *Turris babylonia* (Linnaeus, 1758), *Gemmula kieneri* (Doumet, 1840), *Unedogemmula unedo* (Kiener, 1839) and *Turridrupa* sp. The MolD program (Fedosov *et al.*, 2019) was used to identify unique combinations of diagnostic sites for each delimited species.

SHELL AND RADULA MORPHOLOGY

Radulae were prepared by standard methods (Kantor & Puillandre, 2012) and examined by scanning electron microscopy (JEOL JSM 840A or Tescan VEGA II LSU) at the MNHN. Protoconchs and shells were measured in the standard position and the number of protoconch whorls was counted according to Bouchet & Kantor (2004).

The variation of shell shapes was analysed using their outlines. Initially, we selected shells of sequenced specimens that were not broken, truncated or aberrant. To complete this dataset, we obtained photographs of 20 name-bearing types (corresponding to 21 species names) that were deemed high quality, of which 18 were suitable for morphometric analysis (nearly complete shells). In total, shape acquisition was performed for 197 sequenced specimens, 18 types and eight unsequenced specimens of *Cryptogemma periscelida* (Dall, 1889).

Shell shape was acquired from photographs using a Photoshop CC 2019 script. Outlines were reconstructed with the package Momocs (Bonhomme *et al.*, 2014) in R software. We used elliptical Fourier analysis (Giardina & Kuhl, 1977), which has many advantages over alternative Fourier analyses (Bonhomme *et al.*, 2014), to decompose the closed outlines of the shells into periodic functions. The number of harmonics necessary to describe the shape was selected to reach 99.9% of the cumulative harmonic power, ensuring that the majority of shell shape outlines were considered. Shapes were also checked by eye to ensure that enough complexity was captured. The coefficients obtained were normalized to allow the superposition of the first ellipse and make the shapes comparable. We checked that all the reconstructed outlines were aligned appropriately. A principal components analysis (PCA) was performed on the harmonic coefficients in order to capture an optimal shape variation with a minimal number of principal components (PCs). Finally, a linear discriminant analysis (LDA) was performed to find the linear combination of principal components that maximized differences between specimens from species delimited with DNA. Fourier analysis does not take size into account; only shapes are compared. Given that the size of the shells might provide some discriminatory information, we added the length of each specimen as a variable for the LDA. The appropriate number of PCs to use in the LDA model was chosen carefully to find the optimal equilibrium between maximizing the differences and overfitting. A leave-one-out cross-validation procedure was used to find the number of PC axes leading to the best percentage of species predictions (see Supporting Information, Fig. S1). In order to test whether our species attribution to each molecular species partition was correct, type specimens were not included in the LDA training set but were added subsequently in the LDA morphospace. Another reason not to include the types in the training set was to extract the morphological differences between molecular species without the influence of the morphology of type specimens.

All the material examined for this study is summarized in the (Supporting Information Table S1).

RESULTS

A total of 303 *COI*, 32 28S and 18 12S sequences of *Cryptogemma* were used for this study, of which 255, eight and 16, respectively, were newly obtained. The USNM and ZMMU samples yielded poor DNA quality, making them difficult to sequence with a classical Sanger sequencing approach. Nevertheless, the 12S sequence was obtained for the USNM96485 and USNM123087 paralectotypes of *G. benthima* collected 128 years ago. For the ZMMU paratype, the USNM123092 paralectotype and the USNM83292 lot of *P. carynae*, the *COI* sequence was obtained using the newly designed primers conoCOIintR and conoCOIintF. The USNM123092 lot had previously been sequenced and published by Todd & Rawlings (2014) for the *COI* and 12S fragments (GenBank accession numbers KM218745 and KM218648), despite the fact that the samples were most probably formalin fixed. Nevertheless, sequencing an additional specimen from the same lot was necessary, because the lot might include specimens from different species.

All ABGD, mPTP and GMYC analyses (see Supporting Information, Fig. S2) on the *COI* dataset resulted in the same partition, with eight species hypotheses. Both *COI* and 28S turned out, in this clade, to be appropriate markers for species delimitation, confirming the five *COI*-based species hypothesis [*Cryptogemma praesignis* (Smith, 1895), *Cryptogemma tessellata* (Powell, 1964), *Cryptogemma timorensis* (Tesch, 1915), *Cryptogemma unilineata* (Powell, 1964) and *Cryptogemma powelli* sp. nov.] described by Puillandre *et al.* (2012). However, new 28S sequences were not produced here. The 28S sequencing of *Cryptogemma aethiopica* (Thiele, 1925) and *C. periscelida* failed, but these two species are easily recognizable morphologically and are not genetically close to a sister species, making it less probable that the *COI*-based species hypotheses are incorrect. The case of *C. praesignis* and *Cryptogemma phymatias* (Watson, 1886) could be considered problematic, because they were found to be sister species and were separated bathymetrically. However, the single sequence of 28S recovered for *C. phymatias* (AMS C.571715) showed a divergence from the available 28S sequences of *C. praesignis* comparable to the divergence between other sister species (results not shown herein; see Puillandre *et al.*, 2012, 2017).

For these eight species hypotheses, we searched for all names available and potentially applicable (see also the Taxonomy section). By consulting the relevant literature on Turridae (e.g. Powell, 1964; Tucker, 2004) and by comparison of type specimens or their images with shells of sequenced specimens, we found 23 names (see Taxonomy section) that we applied tentatively to this partition. A total of 18 name-bearing types corresponding to 19 names were of sufficient quality to be included in the morphometric study. The other name-bearing types are discussed and assigned to molecular species using only the shell photographs or drawings and extrinsic parameters, such as the bathymetry or geography (see Taxonomy section).

Despite considerable intraspecific morphological heterogeneity, the morphometric analysis yielded instructive results. Using shape alone, the leave-one-out cross-validation procedure successfully predicted the correct species attribution of 84% of sequenced specimens and confirmed placement of 14 types out of 18 attributed a priori to our species hypotheses (see Supporting Information, Fig. S3). By adding shell size, we increased the score of the leave-one-out cross-validation procedure to 90.64% of the sequenced specimens and 15 out of 18 types (Fig. 1). The three type specimens whose placement was incorrectly attributed a priori were *Bathybermudia carynae* Haas, 1949 (only representative of its species), *Pleurotoma praesignis* Smith, 1895 and *Ptychosyrinx bisinuata japonica* Okutani, 1964 (see also Taxonomy section). The most discriminant axis (Fig. 1, axis 1: 71.92%

of trace) corresponded to the variation range of the siphonal canal length and the width of the shell. Variation along the second axis (15.57% of trace) mainly corresponded to the intensity of the curvature of the outer aperture lip.

The phylogenetic trees resulting from the *COI* (Fig. 2) and concatenated gene analyses (Fig. 3) showed poorly supported interspecific relationships, except for the *Cryptogemma phymatias*/*C. praesignis* sister relationship and the *C. unilineata* + *C. timorensis* + *C. powelli* clade. Thus, the two molecular species, PSH 11 and PSH 14, in the study by Puillandre *et al.* (2012), which were attributed to the genus *Ptychosyrinx*, did not form a monophyletic group. The genera *Cryptogemma* Dall, 1918 (type species: *G. benthima* Dall, 1908), *Ptychosyrinx* Thiele 1925 [type species: *Pleurotoma* (*Subulata*) *bisinuata*
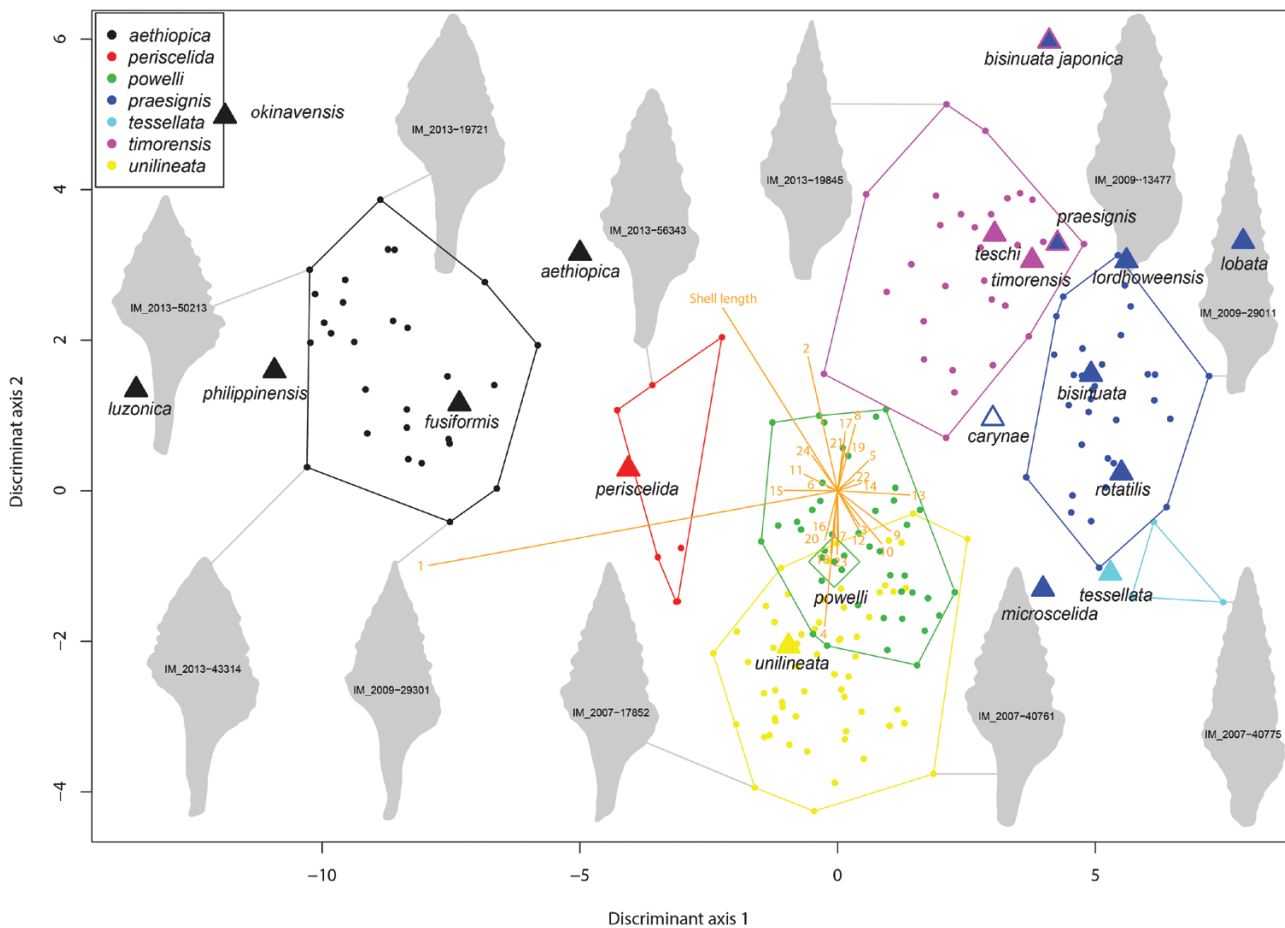

Figure 1. Projection of specimens along the two first discriminant axes. Convex hulls are drawn for easy observation of the range of each species in the morphospace. Triangles are type specimens, with names of species indicated; the background colour corresponds to the species attribution from the literature and the border colour to the linear discriminant analysis (LDA) prediction. Type specimens were not included in the LDA training set. Orange segments correspond to the projection of coefficients multiplied by the standard deviation of each raw variable (principal component axes and shell length). Outlines of the most extreme shapes are drawn with their respective MNHN numbers.
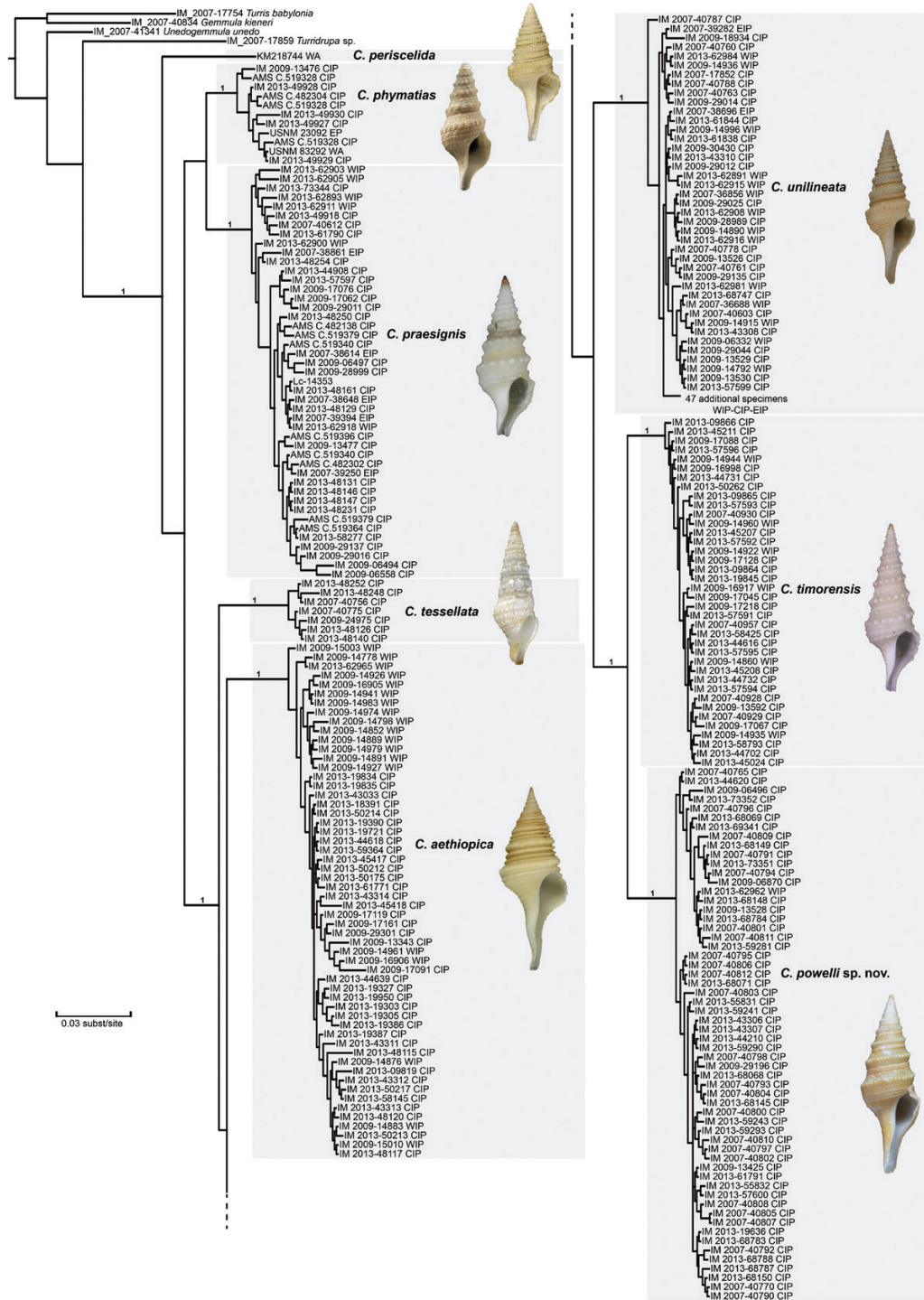
Figure 2. Bayesian tree (MrBayes) for *COI*. Posterior probabilities (> 0.95) are shown only for specific and interspecific nodes. Abbreviations next to each specimen number refer to main marine provinces: CIP, central Indo-Pacific; EIP, eastern Indo-Pacific; EP, eastern Pacific; WA, western Atlantic; WIP, western Indo-Pacific. The alignment is provided in the Supporting Information (Appendix S1).

Martens, 1901] and *Pinguigemmula* McNeil, 1961 (type species: *Pinguigemmula okinavensis* McNeil, 1960), despite being easy to recognize morphologically,

showed a level of molecular divergence among them that was similar to, or even lower than, the level of divergence found among species in most other turrid
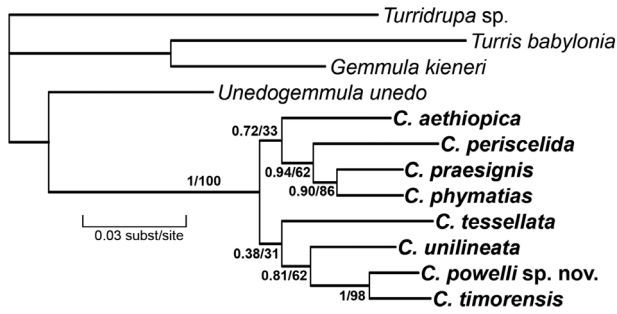
Figure 3. Bayesian tree (MrBayes) of *COI*, 12S and 28S combined. Posterior probabilities and bootstrap values are shown for each node. The alignment is provided in the Supporting Information (Appendix S2).

genera, thus suggesting synonymization of the two latter genera with *Cryptogemma*.

All species showed large, oceanic or transoceanic, sympatric distributions. Despite having largely sympatric distribution, the *C. phymatias*/*C. praesignis* sister species are found in different bathymetric zones, ~1400–3000 and ~300–1400 m, respectively, with the exception of two specimens, one for each species, found at the same station CP2752 (1378–1436 m) during the AURORA 2007 expedition, off Luzon Island, in the Philippines (Supporting Information, Table S1). For all species the geographical (Fig. 4) and depth (Fig. 5) ranges were represented using only sequenced specimens, except for *C. periscelida*, for which the *COI* sequencing did not work for the 13 MNHN samples available, but information on geography and bathymetry was included nonetheless.

TAXONOMY

SUPERFAMILY CONOIDEA FLEMING, 1822

FAMILY TURRIDAE H. & A. ADAMS, 1853 (1838)

GENUS *CRYPTOGEMMA* DALL, 1918

Type species: Gemmula benthima Dall, 1908 (OD).
   Ptychosyrinx Thiele, 1925 (type species: *Pleurotoma bisinuata* Martens, 1901 – OD).
   Bathybermudia Haas, 1949 (type species: *Bathybermudia carynae* Haas, 1949 – OD).
   †*Pinguigemmula* McNeil, 1960 (type species †*Pinguigemmula okinavensis* McNeil, 1960 – OD).

Included species: Cryptogemma aethiopica (Thiele, 1925); *C. periscelida* (Dall, 1889); *C. phymatias* (Watson, 1886); *C. powelli*; *C. praesignis* (Smith, 1895); *C. tessellata* (Powell, 1964); *C. timorensis* (Tesch, 1915); *C. unilineata* (Powell, 1964).

Remarks: According to WoRMS (checked http://www.marinespecies.org/, July 2019), *Cryptogemma* comprises

11 species and has never been revised. A consultation of available type photographs and published images on *Cryptogemma* species indicated that all 11 species, except the type species *C. benthima* and *C. phymatias*, the senior synonym of *C. benthima*, should be excluded from the genus, because the majority of them lack key characters, such as the narrow fusiform shell and the well-marked peripheral anal sinus. Moreover, studied samples from Japan, most certainly corresponding to *Cryptogemma corneus* (Okutani, 1966) as pictured by Hasegawa (2009: figs 335–338), showed closer affinity to other conoidean families (e.g. Horaiclavidae) than to the Turridae, based on both the sequence of the barcode fragment of *COI* and the radular morphology (results not shown). The eight species of *Cryptogemma* listed herein have wide distributions, most of them covering the whole Indo-Pacific tropical region, and are not found at depths shallower than 200 m.

The protoconch consists of four to 5.25 whorls. The shell shape of the teleoconch combined with size is an important factor to distinguish species (see Results section), despite high intraspecific variability. The widest range of variability is observed in shell proportions, with shells with a wide last whorl and long siphonal canal being at one extreme of the range and more elongated shells with short siphonal canal at the other.

CRYPTOGEMMA PHYMATIAS (WATSON, 1886)

(FIG. 6)

Pleurotoma phymatias R. B. Watson, 1886. 1920 m, Philippine Islands, 16°42′N, 119°22′E (Expedition H.M.S. *Challenger* on 13 November 1874, st. 205).
   Gemmula benthima Dall, 1908. 2323 m, Gulf of Panama.
   Gemmula benthina – Dall, 1918: 318 (*lapsus calami*); Powell, 1964: 279 (*lapsus calami*).
   *Pleurotoma truncata* Schepman, 1913. 2798 m, Banda Sea, Indonesia, 6°24′S, 124°39′E.
   Bathybermudia carynae Haas, 1949. 3109 m, off Bermuda, 32°08.2′N, 64°33′W.

Remarks: This species was not present in the sampling of Puillandre *et al.* (2012), but was included in the phylogeny of Puillandre *et al.* (2011) under the name *Ptychosyrinx carynae*.

Owing to the frequent loss of the shell apex, there are few available protoconchs for this species. Only the eroded protoconch of the type specimen of *Bathybermudia carynae* could be measured, with PD = 1.3 mm and PL > 1.6 mm, consisting of more than three whorls.

The radula is of medium length, ~2.6 mm (0.44 of AL), composed of 74 transverse rows of teeth. Marginal teeth are 118–128 μm long (mean 120 μm, *N* = 5), duplex. The
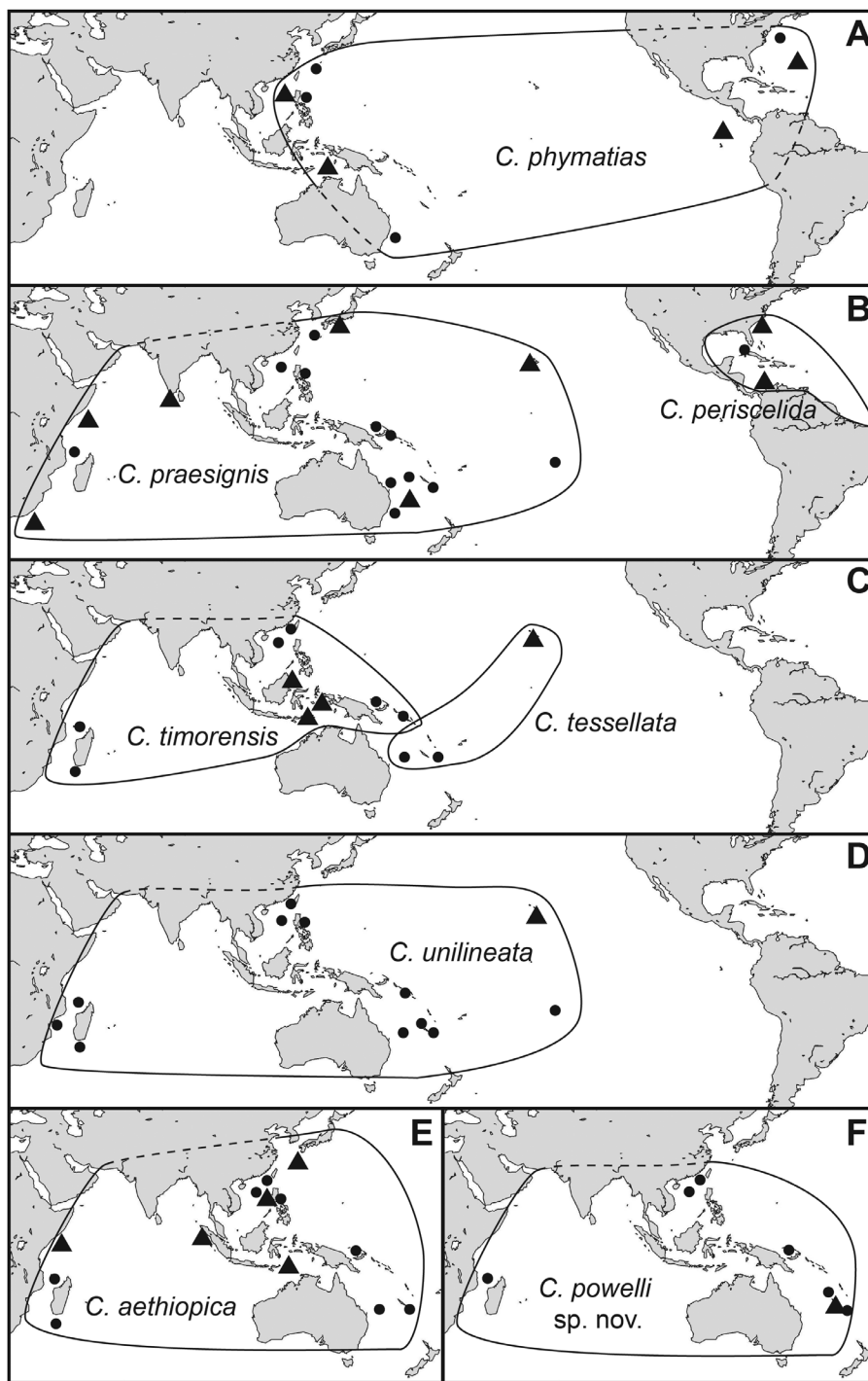
Figure 4. Map showing the species distributions. Filled circles represent localities of sequenced specimens. Full triangles represent localities of type specimens.

anterior (inner) one-third of the tooth length is solid, narrow in dorsal view, pointed; in the posterior two-thirds, major and accessory limbs are broadly bifurcating, and the accessory limb has a clear constriction at about half the tooth length, slightly shorter than the major limb.

The central formation has a distinct narrow carinated cusp and lateral inconspicuous flaps with indistinct lateral and anterior margins (Fig. 7B, C).

Although this species can be distinguished from its congeners by the frequent loss of the first whorls, and
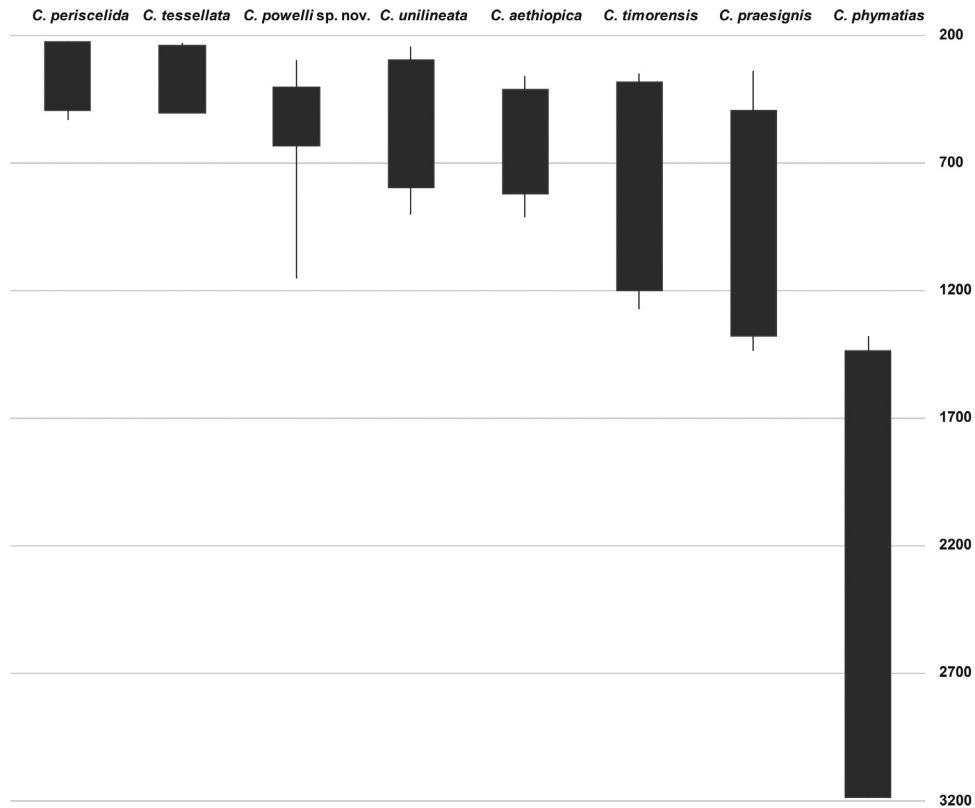
Figure 5. Bathymetric distributions of the eight species. Vertical bars and lines denote 'confirmed' and 'potential' depth ranges, respectively. As a single trawl/dredge haul accumulate samples from a range of depths, the confirmed shallowest of a species is the deepest point of the shallowest haul with the species, and vice versa for the confirmed deepest. Potential ranges are from the shallowest point of the shallowest haul to the deepest of the deepest haul.

from its sister species *Cryptogemma praesignis* by the slightly larger diameter of the shell, the bathymetry is its most distinct characteristic. *Cryptogemma praesignis* is found between ~300 and ~1400 m depth, whereas *C. phymatias* is the only Turridae, to our knowledge, to be found exclusively below ~1400 m deep. Moreover, it is the only Turridae so far, and possibly the first reported benthic gastropod, to have a Pacific–Atlantic distribution (Fig. 4; see Discussion). Most studied type specimens have eroded shells, but the variability of the last whorls, siphonal twist and aperture among them agrees with the variability in the sequenced specimens. Note that the etymology of this species combines '*Cryptogemma*' (hidden gems) and '*phymatias*' (one who has tubercules), resulting in a confusing combination.

List of COI *diagnostic sites (position: character state):* [379: T; 493: C; 622: C]. Indexing starts right next to the 3′ end of the LCO1490 primer (from 1 to 658).

Distribution: From the central Indo-Pacific (Banda Sea) to the North Atlantic Ocean (Bermuda Island) (Fig. 4A),

from a depth of ~1400 to ~3000 m (Fig. 5). This species is expected to be found in the Indian Ocean, as is the case with other Indo-Pacific species of *Cryptogemma*, but it has not been documented there, presumably owing to a lack of sampling at bathyal depths.

CRYPTOGEMMA PRAESIGNIS (SMITH, 1895)

(FIG. 8A–K)

*Pleurotoma praesignis* Smith, 1895. 1234 m, off Colombo, Ceylon [Sri Lanka].

? *Pleurotoma microscelida* Dall, 1895. 642 m, South of Oahu Island Albatross st. 3475, Hawaii.

Pleurotoma (*Subulata*) *bisinuata* Martens, 1901. 1134 m, off East Africa, 1°49′N, 45°29′E.

Pleurotoma rotatilis Martens, 1902. 1134 m, off Mogadishu, Somalia, East Africa, 1°49′N, 45°29′E.

Pleurotoma (*Surcula*) *lobata* G. B. Sowerby III, 1903. 805 m, off Cape Natal, Durban and 567 m, off Buffalo River, East London, S. Africa. E. A. Smith, 1906.

*Ptychosyrinx bisinuata japonica* Okutani, 1964. 620 m, Sea of Enshu-nada, Japan, 34°25.7′N, 137°58.5′E.
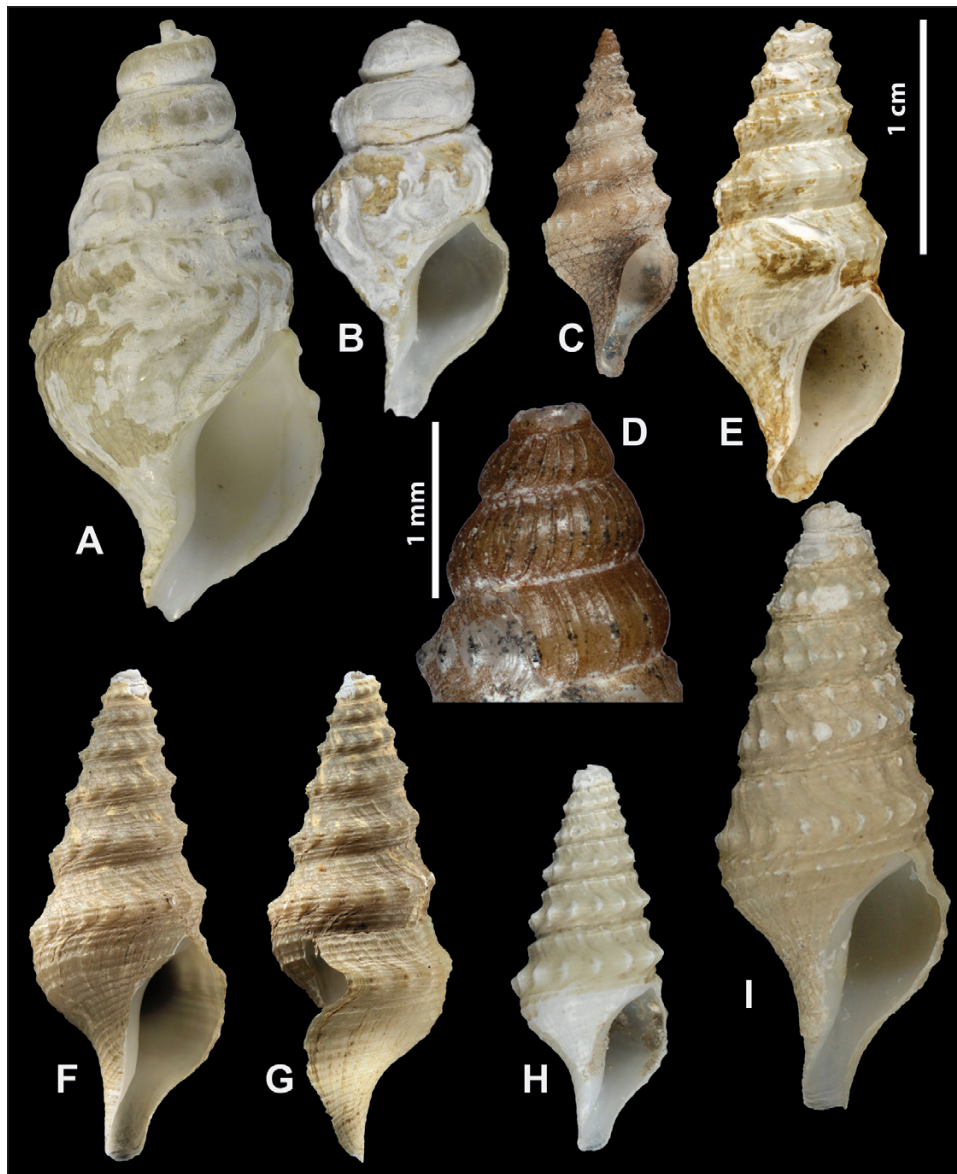
Figure 6. *Cryptogemma phymatias* (Watson, 1886). A, lectotype of *Gemmula benthima* Dall, 1908, USNM 123089, Gulf of Panama. B, paralectotype of *G. benthima* Dall, 1908, USNM 123087, Gulf of Panama. C, holotype of *Bathybermudia carynae* Haas, 1949, FMNH 31656, Bermuda. D, lateral view of the protoconch of *B. carynae*. E, holotype of *Pleurotoma phymatias* Watson, 1886, NHMUK 1887.2.9.957, Philippines. F, G, AMS C.482304, IN2017_V03 – Sampling the Abyss, Jervis Commonwealth Marine Reserve. H, MNHN-IM-2013-49928, R/V Tansei-maru, KT-12–32, Okinawa. I, MNHN-IM-2009-13476, AURORA 2007, Philippines.

Ptychosyrinx lordhoweensis Kantor & Sysoev, 1991: 205, figs 1, 2. 1210 m, Lord Howe Rise, off eastern Australia, 30°24′S, 161°51′E.

Remarks: This species corresponds to PSH 11 in the study by Puillandre *et al.* (2012).

The protoconch exhibits a wide size range, with PD = 1.05–1.38 mm and PL = 1.4–1.93 mm, and from four to 5.2 whorls.

The radula is long, ~3.4 mm in length (0.44 of AL), formed of 72 transverse rows of teeth. The marginal teeth are 142–151 μm long (mean 149 μm, $N = 5$, or 1.9% of AL), duplex. The anterior (inner) one-third of the tooth length is solid, narrow in dorsal view, pointed; in the posterior two-thirds the major and accessory limbs are broadly bifurcating, and the accessory limb has a clear constriction and is bent at about half tooth length, shorter than the major limb. The central
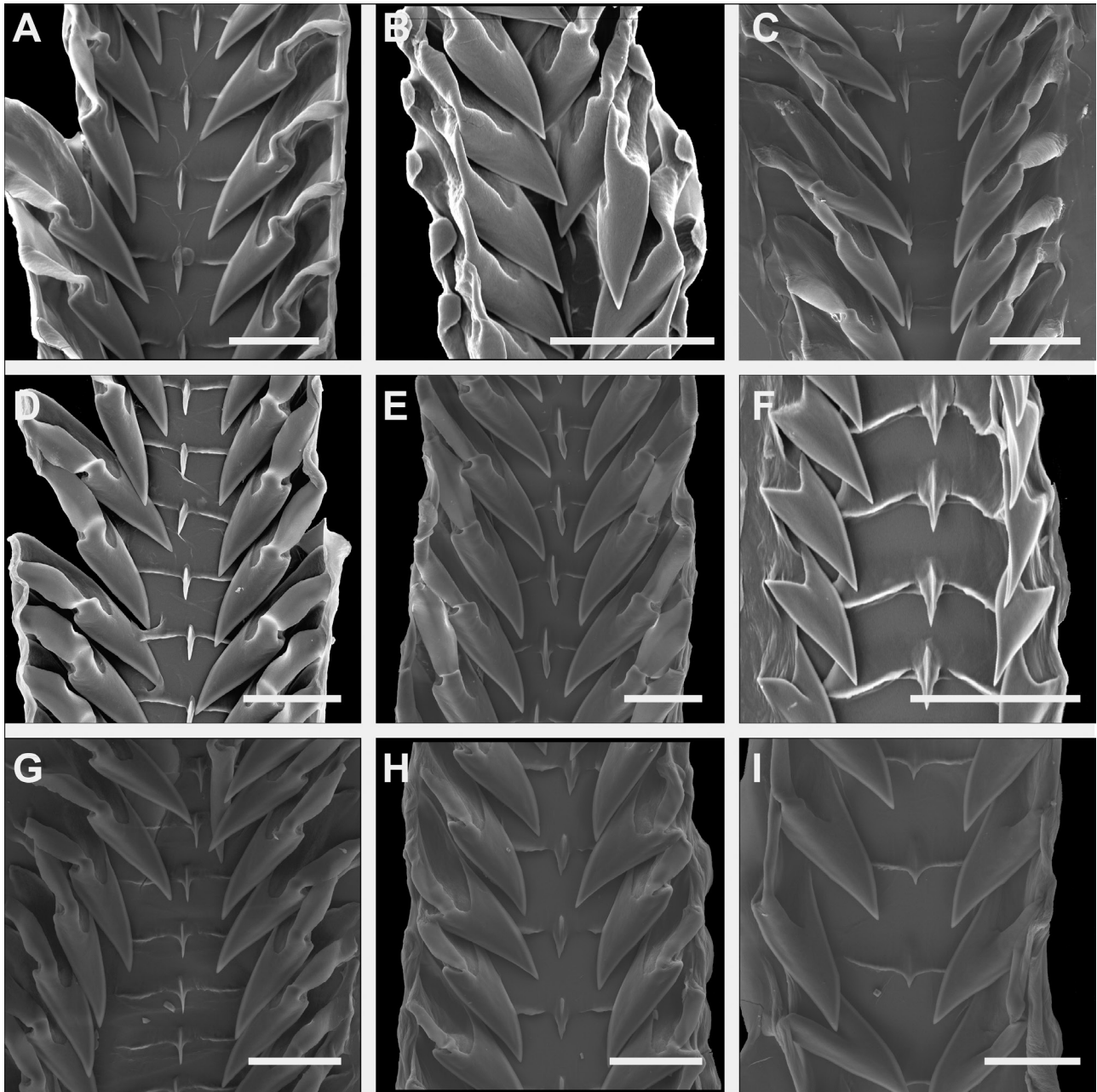
Figure 7. Radulae of studied *Cryptogemma*. A, *Cryptogemma praesignis* (Smith, 1895). B, C, *Cryptogemma phymatias* (Watson, 1886). B, MNHN uncatalogued, BIOCAL, New Caledonia, st. CP23. C, USNM 857019, Venezuela. D, *Cryptogemma periscelida* (Dall, 1889), R/V *Pelican*, 28°23.935′N, 89°22.508′W, 675–765 m. E, *Cryptogemma aethiopica* (Thiele, 1925), MNHN-IM-2013-50175, DONGSHA 2014, Taiwan. F, *Cryptogemma tessellata* (Powell, 1964), MNHN-IM-2007-40775, EBISCO, Chesterfield Islands. G, *Cryptogemma unilineata* (Powell, 1964), MNHN-IM-2013-61844, ZHONGSHA 2015, Taiwan. H, **Cryptogemma powelli**, MNHN-IM-2013-68787, KANACONO, New Caledonia. I, *Cryptogemma timorensis* (Tesch, 1915), MNHN-IM-2013-09864, PAPUA NIUGINI, Papua. Scale bars: 50 μm.

formation has a distinct narrow carinated cusp and lateral inconspicuous flaps with indistinct lateral and anterior margins (Fig. 7A).

This species is morphologically close to *C. timorensis*, although it differs from that species in its generally smaller size (~15–35 mm SL), in having a narrower last whorl and in the presence of a tertiary apertural notch in mature females. *Cryptogemma praesignis* also differs from *C. timorensis* in having a much longer radula (0.44 vs. 0.2 of AL) and relatively longer
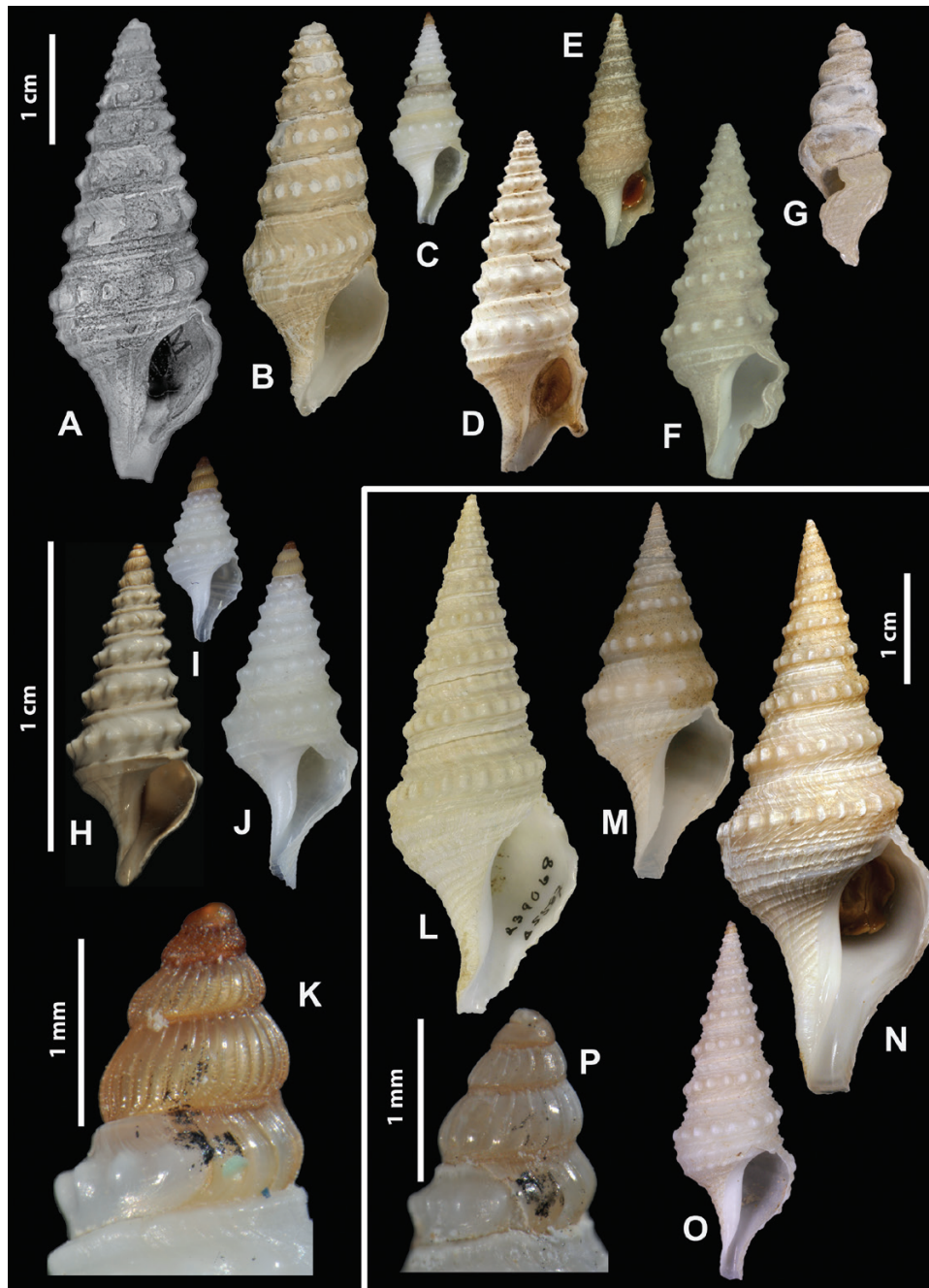
Figure 8. *Cryptogemma praesignis* (Smith, 1895) (A–K) and *Cryptogemma timorensis* (Tesch, 1915) (L–P). A, holotype of *Pleurotoma praesignis* Smith, 1895, ZSIC, Sri Lanka. B, MNHN-IM-2009-13477, AURORA-2007, Philippines. C, MNHN-IM-2013-62903, BIOMAGLO, Iles Glorieuses. D, holotype of *Pleurotoma lobata* Sowerby III, 1903, NHMUK 1903.7.27.49, South Africa. E, holotype of *Ptychosyrinx lordhoweensis*, ZMMU Lc-14532, Lord Howe Rise. F, syntype of *Pleurotoma bisinuata* von Martens, 1901, ZMB 683, off East Africa. G, holotype of *Pleurotoma microscelida* Dall, 1895, USNM 127122, Hawaiian Islands. H, holotype of *Pleurotoma rotatilis* von Martens, 1902, ZMB 60070, off East Africa. I, MNHN-IM-2013-62893, BIOMAGLO, Iles Glorieuses. J, MNHN-IM-2013-62900, BIOMAGLO, Iles Glorieuses. K, lateral view of the protoconch of MNHN-IM-2013-62893. L, holotype of *Ptychosyrinx timorensis teschi* Powell, 1964, USNM 239068, Borneo. M, MNHN-IM-2009-14860, ATIMO VATAE, south of Madagascar. N, MNHN-IM-2007-40928, SALOMON 2, Solomon Islands. O, MNHN-IM-2013-58793, KAVIENG, Papua. P, lateral view of the protoconch of MNHN-IM-2009-14935.

marginal teeth (1.9% of AL vs. 1.35%). Anatomical examination of Australian material (AMS C.571714 and AMS C.571704) shows that mature males (SL 29.4 and 34.9 mm, respectively) may possess extremely large and muscular penis, with a width almost equal to the width of the animal itself and with a large, long, lateral appendage situated distally. The penial tip is rather blunt, with the opening situated distally. A third, smaller Australian specimen (AMS C.571757; SL 25.7 mm) did not possess a well-developed papilla, suggesting that such a feature might develop with increasing maturity and therefore not be present in subadults. Furthermore, the shells of AMS C.571714 and AMS C.571704 did not possess a tertiary apertural notch. The observation of AMS C.571714 and AMS C.571704 supplements the findings of Kantor & Sysoev (1991) that the mature females of this species develop a tertiary apertural notch. The authors hypothesized that this structure was possibly connected with the process of fertilization. Such a feature has also been observed in *C. aethiopica* specimens (Fig. 9G, I), but not in other *Cryptogemma* species.

The general morphology and, more specifically, the presence of a tertiary apertural notch in *Pleurotoma bisinuata* and *Ptychosryinx bisinuata japonica* supports the synonymization of these names with *C. praesignis*. Given that the holotype of *P. bisinuata japonica* is a comparatively large specimen (39 mm), the result of the
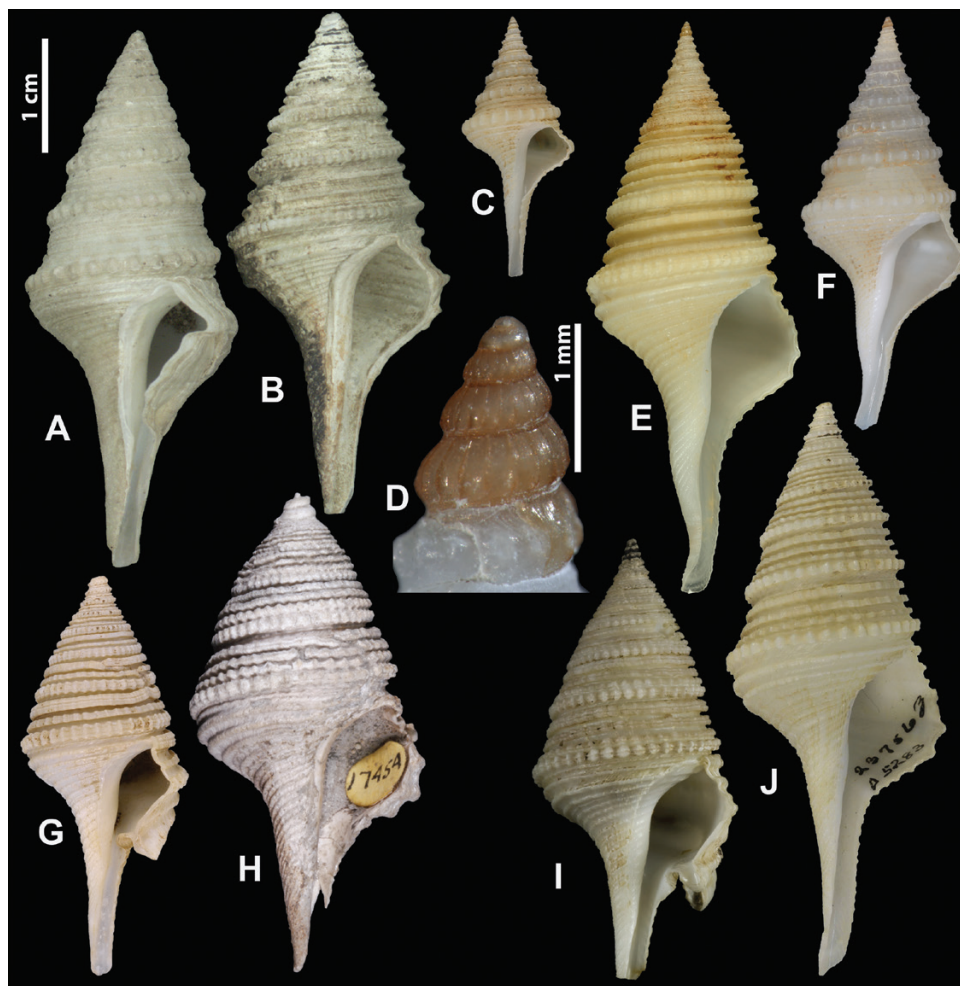
Figure 9. *Cryptogemma aethiopica* (Thiele, 1925). A, holotype of *Pleurotoma aethiopica* Thiele, 1925, ZMB 109376, off East Africa. B, holotype of *Pleurotoma fusiformis* Thiele, 1925, ZMB 109388, off Sumatra. C, MNHN-IM-2009-14979, ATIMO VATAE, South of Madagascar. D, lateral view of the protoconch of MNHN-IM-2013-48115, KANADEEP, Chesterfield Islands. E, MNHN-IM-2009-29301, EXBODI, New Caledonia. F, MNHN-IM-2009-14778, ATIMO VATAE, South of Madagascar. G, holotype of *Pinguigemmula luzonica* Powell, 1964, USNM 237784, Philippines. H, holotype of *Pinguigemmula okinavensis* McNeil, 1960, UNSM MO 562851, Miocene or Pliocene of Okinawa. I, MNHN-IM-2013-19950, PAPUA NIUGINI, Papua. J, holotype of *Pinguigemmula philippinensis* Powell, 1964, USNM 237563, Philippines.

LDA and the leave-one-out cross-validation procedure attributed it to *C. timorensis*. Possibly for the same reason, the holotype of *P. praesignis* (42 mm) also fell into the *C. timorensis* range. The result of the LDA and the leave-one-out cross-validation procedure when considering only shape predicted the two holotypes as *C. praesignis* (see Supporting Information, Fig. S3), thus justifying the attribution of *P. praesignis* to this molecular species. The sequencing of a paratype of *Ptychosyrinx lordhoweensis* confirmed its conspecificity with *C. praesignis*. *Pleurotoma lobata*, although conchologically similar to *P. bisinuata*, has never been synonymized based on the reportedly different morphology of the radula: the absence of a central tooth (= central formation as understood herein) in the specimens of *P. lobata* examined by Barnard (1958), contrasting with the large unicuspid rectangular-based central tooth described in *P. bisinuata* by Thiele (1929: 359). Powell (1964) suggested that Thiele could have mixed his radula preparations, but in light of the types of radulae of *Cryptogemma* (Fig. 8), all composed of a unicuspid central formation, it is more likely either that it was Barnard who mixed up the radula preparation or that the specimens examined by Barnard are not *Cryptogemma* specimens. The holotype of *Pleurotoma rotatilis* is almost identical conchologically to a sequenced juvenile from the East African coast (MNHN-IM-2013-62900; Fig. 8J). Some doubts remain regarding the status of *Pleurotoma microscelida*, but the size and overall last whorl morphology of the type specimen show a stronger resemblance to *C. praesignis* than to any other *Cryptogemma* species.

List of COI *diagnostic sites (position: character state):* [232: A; 319: T; 407: C; 409: T].

Distribution: This species is known to occur from the western Indian Ocean to the eastern Pacific Ocean (Fig. 4B), from a depth of ~300 to ~1400 m (Fig. 5).

CRYPTOGEMMA TIMORENSIS (TESCH, 1915)

(FIG. 8L–P)

†*Pleurotoma timorensis* Tesch, 1915. Timor. Pliocene.
    †*Pleurotoma ktolemandoënsis* K. Martin, 1933. Ktolemando. Miocene.
    Ptychosyrinx timorensis teschi Powell, 1964: 291 (22–853), pl. 223, figs 5, 6. 759 m, north-west off Sipadan Island, Borneo.

Type locality: Pliocene of Timor Island.

Remarks: This species corresponds to PSH 14 of Puillandre *et al.* (2012).
    Protoconch commonly eroded, with PD = 1–1.2 mm and PL = 1.3–1.675 mm and number of whorls varying from four to 4.5.

The radula is medium short, ~2.5 mm in length (0.2 of AL), formed of 45 transverse rows of teeth. Marginal teeth are 162–172 µm long (mean 168 µm, $N = 5$, or 1.35% of AL), duplex. Anterior (inner) one-third of the tooth length is solid, medium broad in dorsal view, lanceolate; in posterior two-thirds the major and accessory limbs are broadly bifurcating, the accessory limb with a clear constriction and bent at about half tooth length, nearly the same length as the major limb. The central formation has a short and obtuse cusp and lateral inconspicuous flaps with indistinct lateral and anterior margins. The posterior margin is thickened and uninterrupted along its length (Fig. 7I).

The type of this species is a fossil specimen from Timor island (Indonesia/Timor Leste) described by Tesch (1915), and Martin (1935) described another similar specimen from Buton island (Indonesia) as *Pleurotoma ktolemandoënsis*, without reference to the work of Tesch. However, Martin (1935) also recognized the affinities between *Pleurotoma timorensis* and *Pleurotoma ktolemandoënsis*. Finally, Robba *et al.* (1989) synonymized *Pleurotoma ktolemandoënsis* with *Pleurotoma timorensis*. Powell (1964) described the subspecies *Ptychosyrinx timorensis teschi* based on an extant specimen, which Sysoev (1996) elevated to species rank. The argument by both authors for separating the fossil species from the extant species was the 'much broader' shell of the extant *Ptychosyrinx timorensis teschi* specimen. Examination of the morphological variability of the sequenced specimens shows that the dimensions and shape of fossil specimens are close to the inferred average breadth of the species; some specimens show a broader aperture and a taller last whorl than others, despite having the same number of teleochonch whorls. The results of the LDA show that *Pleurotoma timorensis* and *Ptychosyrinx timorensis teschi* fall within the variability of the sequenced specimens. The broader last whorl and the generally larger size (~30–55 mm) are characteristic for *C. timorensis* when compared with *C. praesignis*.

List of COI *diagnostic sites (position: character state):* [73: G; 214: G; 334: G; 511: G].

Distribution: Found from the western Indian Ocean to the central Indo-Pacific (Fig. 4C), from a depth of ~300 to ~1200 m (Fig. 5). Curiously, this species has not been found in New Caledonia, despite considerable sampling effort in this region.

CRYPTOGEMMA AETHIOPICA (THIELE, 1925)

(FIG. 9)

Pleurotoma aethiopica Thiele, 1925. 638 m, off Somalia, East Africa, 0°27′S, 42°47.3′E. (Expedition Deutschen Tiefsee, st. 253).

Pleurotoma fusiformis Thiele, 1925. 614 m, Niassüdkanal, 0°15.2′N, 98°08.8′E.

Gemmula thielei Finlay, 1930. (nom. nov. for *Pleurotoma fusiformis* Thiele, 1925).

†*Pleurotoma trincincta* Martin, 1935: 113, pl. 2, figs 2, 2a. Buton Island, south-east Celebes. Oligocene.

†*Pinguigemmula okinavensis* McNeil, 1960. Okinawa. Japan, Shinzato Tuff Member, Miocene or Pliocene.

Pinguigemmula luzonica Powell, 1964: 278(22–790), pl. 215, figs 3, 4. 326 m, off Hermana, Menor Island, Luzon Island, Philippines.

Pinguigemmula philippinensis Powell, 1964: 278(22–790), pl. 215, figs 5, 6. 512 m, off Santiago, west Luzon Island, Philippines.

Remarks: This species was not included in the study by Puillandre *et al.* (2012). The protoconch is commonly eroded, with PD = 1.05–1.25 mm, PL = 1.375–1.75 mm and number of whorls ranging from 4.2 to five.

The radula is long, ~3.4 mm in length (0.37 of AL), composed of 77 transverse rows of teeth. The marginal teeth are 150–159 µm long (mean 155 µm, N = 5, or 1.66% of AL), duplex. The anterior (inner) 0.4 of the tooth length is solid, narrow in dorsal view, awl shaped; in the posterior part the major and accessory limbs are broadly bifurcating, the accessory limb with a clear constriction and bent at about half tooth length, thin, nearly same length as the major limb. The central formation has a long, narrow, sharp, carinated cusp and lateral flaps with distinct posterior and anterolateral margins. The flaps are not completely fused with the cusp (Fig. 7E).

The former genus *Pinguigemmula* is easily distinguishable from *Gemmula* in having a broadly conical spire, a strongly constricted base and a long, straight siphonal canal (Powell, 1964). Although expressing a broad variety of forms, the molecular analysis resulted in a single species hypothesis. Several species were described based on the sculptural details, such as the number of gemmate cords (one, two or none). The sculpture seems to be correlated with geography, with the forms from the western Indian Ocean having a smooth intersuture sculpture, whereas the forms from the eastern Indian Ocean to the western Pacific Ocean usually possess two or three gemmate cords. Some large specimens of this species have a similar 'tertiary notch' to that of *C. praesignis*, suggesting sexual dimorphism also for this species (Kantor & Sysoev, 1991).

List of COI *diagnostic sites (position: character state):* [115: C; 307: A; 418: G].

Distribution: Found off East Africa to the central Indo-Pacific (Fig. 4E), from a depth of ~400 to ~850 m (Fig. 5).

CRYPTOGEMMA TESSELLATA (POWELL, 1967)

(FIG. 10A–D)

Gemmula tessellata Powell, 1967: 439 (22–734a), pl. 315. 183–219 m, off Waikiki, Oahu Island, Hawaiian Islands (collected by Dr Pat Burgess).

Remarks: This species corresponds to PSH 12 in the study by Puillandre *et al.* (2012). The protoconch of the holotype is 4.5 whorls according to Powell (1967), and PD = 1.22 mm and PL = 1.64 mm according to measurements inferred from photographs of the holotype. The protoconch exhibits high variability, with PD = 1.175–1.3 mm, PL = 1.525–1.975 mm and consisting of four to 5.5 whorls.

The radula is of medium length, ~1.2 mm (0.29 of AL), composed of 51 transverse rows of teeth. The marginal teeth are 86–91 µm long (mean 89 µm, N = 2, or 2.1% of AL), duplex. The anterior (inner) half of the tooth length is solid, medium broad in dorsal view, triangular. The accessory limb is weak, thin, without constriction, much shorter than the major limb, but of nearly same width (the marginal teeth in Fig. 8F are not fully sclerotized). The central formation has a long, sharp and carinated central cusp, slightly curved in profile, and with lateral conspicuous flaps with distinct margins. The flaps are not completely fused with the cusp. The anterior margin of the central formation is strongly concave (Fig. 7F).

The 'light form' of *C. tessellata* has been misidentified by Puillandre *et al.* (2012) as *Xenuroturris gemmuloides* Powell, 1967 because it shares superficially similar features, such as the white-yellowish shell punctuated with regular brown-orange spots, and the small size (~15–25 mm). The 'brown-orange form' of *C. tessellata*, closer to the holotype, is distinctly different from the 'light form' not only in colouration, but also in having a stouter outline and a more tuberculate subsutural fold (Powell, 1967). Although readily distinguished from the other *Cryptogemma* species owing to its colour pattern and small size, LDA indicates that this species more closely resembles small adults of *C. praesignis*.

List of COI *diagnostic sites (position: character state):* [46: C; 61: A; 316: T].

Distribution: The sequenced specimens were found off New Caledonia only, and the holotype is from the Hawaiian Islands (Fig. 4C), from a depth of ~200 to ~500 m (Fig. 5). The protoconch characteristics, similar in shape, size and number of whorls to *C. praesignis*, imply that the species might have a much broader range than what is currently documented, possibly covering the entire central Pacific.
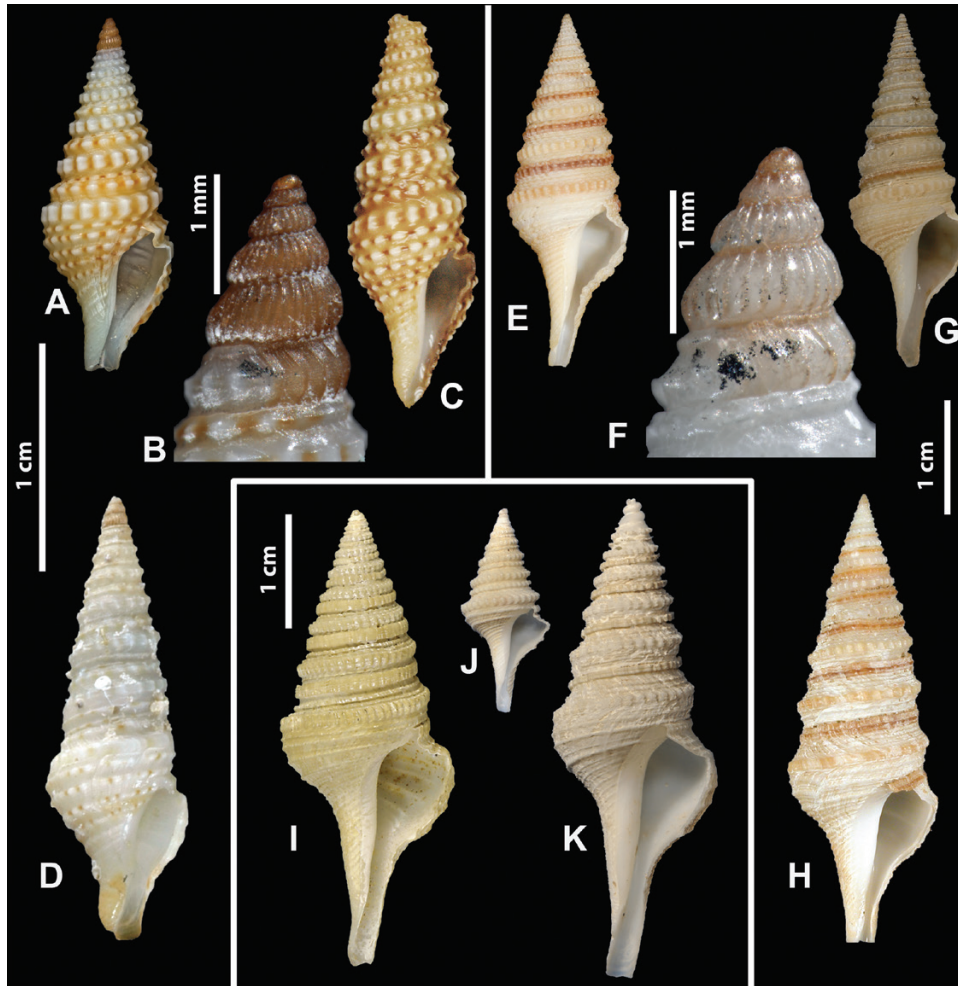
Figure 10. *Cryptogemma tessellata* (Powell, 1967) (A–D), *Cryptogemma unilineata* (Powell, 1964) (E–H) and *Cryptogemma periscelida* (Dall, 1889) (I–K). A, holotype of *Gemmula tessellata* Powell, 1964, AWMM MA71042, Hawaiian Islands. B, lateral view of the protoconch of MNHN-IM-2013-48252, KANADEEP, Chesterfield Islands. C, MNHN-IM-2009-24975, EXBODI, New Caledonia. D, MNHN-IM-2007-40775, EBISCO, Chesterfield Islands. E, holotype of *Gemmula congener unilineata* Powell, 1964, BPBM 8929, Hawaiian Islands. F, lateral view of the protoconch of MNHN-IM-2007-40786, NORFOLK 2, New Caledonia. G, MNHN-IM-2009-14953, ATIMO VATAE, south of Madagascar. H, MNHN-IM-2007-38340, MAINBAZA, Mozambique channel. I, lectotype of *Pleurotoma periscelida* Dall, 1889, USNM 87391, Colombia. J, MNHN-IM-2013-56285, GUYANE 2014, French Guiana. K, MNHN-IM-2013-56283, GUYANE 2014, French Guiana.

CRYPTOGEMMA UNILINEATA (POWELL, 1967)

(FIG. 10E–H)

Gemmula congener unilineata Powell, 1967: 437(22–716a), pl. 313. 366 m, off Waikiki, Oahu Island, Hawaii (Expedition Pele, 13 June 1964).

Remarks: This species corresponds to PSH 13 in the study by Puillandre *et al.* (2012).

The protoconch is commonly retained, with PD = 1.075–1.275 mm, PL = 1.375–1.925 mm and the number of whorls ranging from 4.75 to 5.5.

The radula is long, ~3 mm in length (0.31 of AL), composed of 99 transverse rows of teeth. The marginal teeth are 121–127 µm long (mean 125 µm, N = 5, or 1.27% of AL), duplex. The anterior (inner) 0.4 of the tooth length is solid, narrow in dorsal view and awl shaped. In the posterior part, the major and accessory limbs are broadly bifurcating, the accessory limb with a clear constriction and bent at about half the tooth length, slightly shorter than the major limb. The central formation has a long, sharp, carinated cusp and lateral flaps with distinct posterior and anterolateral margins. The flaps are not completely fused with the cusp (Fig. 7G).

This species has been named based on the characteristic carinated brown-orange subsutural band. The brown-orange subsutural band has been found in *C. powelli* and in some specimens of *C. praesignis*, and in other Turridae, such as *Gemmula cosmoi* (Sykes, 1930), but it is generally smoother and thinner than that of *C. unilineata*. The LDA indicated that *C. unilineata* generally has a more angulated shape on the outer aperture lip of the last whorl, indicating a more concave subsutural ramp in comparison to other *Cryptogemma*. However, we note that the convex hulls (Fig. 1) of *C. unilineata* and *C. powelli* are greatly overlapping; therefore, the strong carinated brown-orange subsutural band remains the best-suited character for distinguishing *C. unlineata* from *C. powelli*.

List of COI *diagnostic sites (position: character state):* [172: G; 307: T; 361: G; 370: C].

Distribution: From East Africa to the central Pacific (Hawaiian and Society Islands) (Fig. 7D), from ~300 to ~800 m deep (Fig. 5).

CRYPTOGEMMA PERISCELIDA (DALL, 1889)

(FIG. 10I–K)

Pleurotoma periscelida Dall, 1889. 283 m (USS *Albatross* expedition, st. 2143, collected on 23 March 1884) and 196 m, off Hatteras, North Carolina.

Remarks: The protoconch is unknown, because it is consistently eroded in all examined material, even in younger specimens.

The radula is of medium length (part of youngest section lost), > 1.9 mm (> 0.22 of AL), composed of > 50 transverse rows of teeth. The marginal teeth are 107–116 µm long (mean 110 µm, *N* = 5 or 1.25% of AL), duplex. The anterior (inner) 0.4 of the tooth length is solid, narrow lanceolate in dorsal view. In the posterior part, the major and accessory limbs are medium broadly bifurcating, and the accessory limb has a clear constriction and is bent at less than half tooth length, thin, nearly the same length and width as major limb. The central formation has a long, narrow, sharp carinated cusp and lateral flaps with distinct posterior and posterolateral margins. The flaps are completely fused with the cusp (Fig. 7D).

This species has been described from the Gulf of Mexico, although specimens from Suriname and from the MNHN recent expedition GUYANE 2014 (French Guiana) were also collected. This is the only '*Gemmula*'-like species to be found exclusively in the Atlantic Ocean, where it occurs in a depth range of 200–800 m.

List of COI *diagnostic sites (position: character state):* [352: C, 412: G, 655: C].

Distribution: Found in the Gulf of Mexico, north to the Carolina coast and south to French Guiana (Fig. 4B), from a depth of ~200 to ~500 m (Fig. 5).

CRYPTOGEMMA POWELLI SP. NOV.

(FIG. 11)

urn:lsid:zoobank.org:act:EC0DAF2A-AD02-4D9D-8970-B49A70385A0A

Type material: Holotype MNHN-IM-2013-68787; paratype 1, MNHN-IM-2007-40795; paratype 2, MNHN-IM-2007-40765; all live collected and processed for DNA extraction.

Type locality: New Caledonia, south-west of Ile des Pins, 22°48′S, 167°15′E, 449–465 m depth, sand and debris (Expedition KANACONO, st. DW4697).

Etymology: Named after New Zealand malacologist Arthur William Baden Powell CBE (1901–1987), who contributed enormously to the systematics of Conoidea and, in particular, who revised the family Turridae in 1964 and described several species of *Cryptogemma*.

Description (holotype): Shell narrowly fusiform, with high spire and medium-long siphonal canal. Protoconch conical, eroded, with a diameter of 1.125 mm, of about four convex whorls. Teleoconch of nine whorls; suture shallow, impressed. Shell height 38 mm, aperture height 10.9 mm and shell diameter 12.5 mm. Whorls strongly shouldered, with slightly concave shoulder slope, very weakly convex, nearly cylindrical periphery. Spiral sculpture of fine, broadly spaced, wavy, subequal spiral cords on subsutural ramp, ten on last whorl, uppermost being much more pronounced than the others, coloured light orange-brown. Sinus cord strongly gemmate, with gemmules clearly bisected (39 on the body whorl). Spiral cords becoming thicker on whorl periphery, sometimes nodulose, some notably wider than others. Axial sculpture of fine growth lines. Last whorl shortly constricted to long siphonal canal, with 32 cords below the sinus, of which ~20 on canal. Aperture irregular oval, outer lip thin, simple. Anal sinus moderately deep, U-shaped. Shell colour straw-yellow, subsutural cord orange-brown, gemmae slightly lighter than background.

Radula medium long, ~3.1 mm in length (0.28 of AL), composed of 75 transverse rows of teeth. Marginal teeth 129–135 µm long (mean 133 µm, *N* = 5 or 1.22% of AL), duplex. Anterior (inner) one-third of tooth length solid, lanceolate in dorsal view, in posterior part major and accessory limbs broadly bifurcating; accessory limb with clear constriction at half tooth length, thin, about half the length and width of the
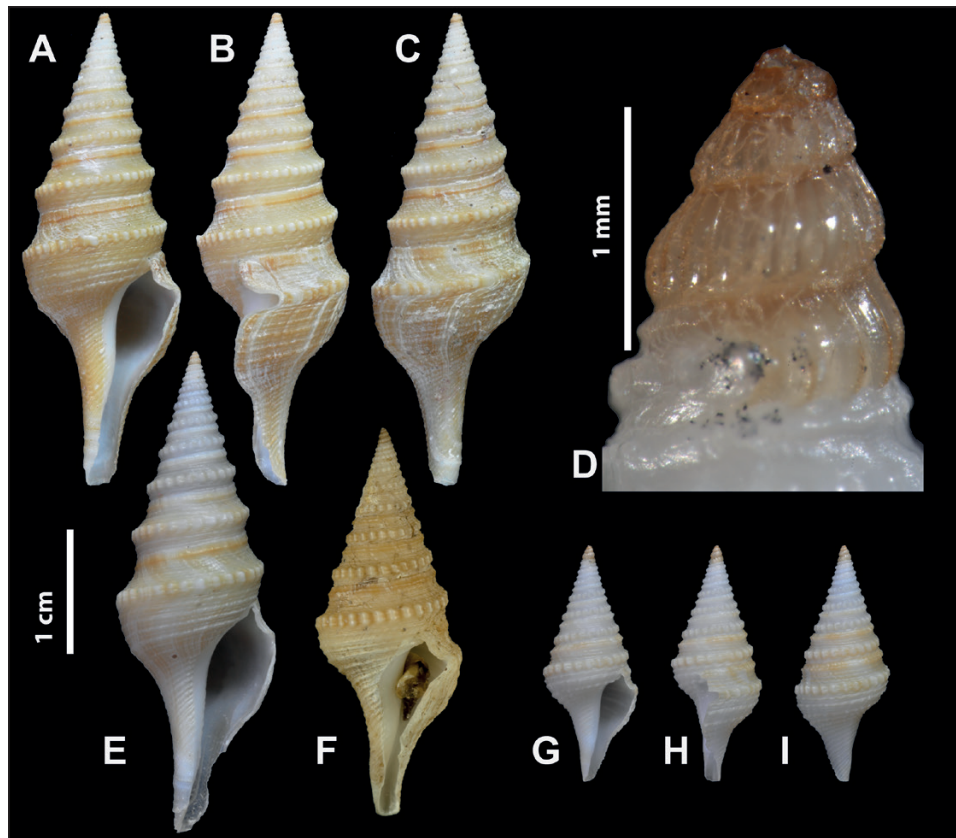
Figure 11. *Cryptogemma powelli*. A–C, holotype, MNHN-IM-2013-68787, KANACONO, New Caledonia. D, lateral view of the protoconch of the paratype 2 MNHN-IM-2007-40765, EBISCO, Chesterfield Islands. E, paratype 1, MNHN-IM-2007-40795, NORFOLK 2, New Caledonia. F, MNHN-IM-2013-55832, TAIWAN 2013, Taiwan. G–I, paratype 2, MNHN-IM-2007-40765, EBISCO, Chesterfield Islands.

major limb. Central formation with medium long and medium broad sharp carinated cusp and lateral flaps with distinct posterior and posterolateral margins. Flaps not completely fused with cusp (Fig. 7H).

Remarks: This species corresponds to PSH 15 in the study by Puillandre *et al.* (2012). *Cryptogemma powelli* exhibits similar intraspecific variation in shell shape to that of its congeners, based on its convex hull area (Fig. 1). Studied specimens vary in shades of shell colour, from light yellowish to light orange, occasionally with a patchy pattern. In terms of both size and shape, *C. powelli* can, in some cases, be undistinguishable from *C. unilineata* (Fig. 1). The morphometric analysis shows considerable overlap of the measured shell features between the two species, with the main distinction between them expressed by the second axis. Interpretation of this result suggests that the *C. powelli* on average possesses a more concave curvature of the outer aperture lip, in comparison to *C. unilineata*. Besides, distinction of *C. powelli* and *C. unilineata* mostly relies on the degree of pronunciation of the

subsutural cord; it is typically not significantly stronger than the succeeding cords in the former species, but is always thick and gemmate in the latter. However, the subsutural cord is thicker in younger specimens, rendering the distinction of juvenile *C. powelli* and *C. unilineata* specimens problematic.

List of COI *diagnostic sites (position: character state):* [112: G; 322: T; 433: A].

Distribution: The confirmed distribution of this species based on sequenced specimens ranges from the Indian Ocean to the central Pacific (Fig. 4F), from a depth of ~400 to ~600 m.

DISCUSSION

Using an integrative taxonomy approach, by combining DNA-based species delimitation methods with classical morphological taxonomic methods, we re-evaluated the *Cryptogemma* group studied by Puillandre *et al.* (2012)

with new sequences, in some cases from type material, resulting in eight delimited species. Among the eight delimited species, *C. phymatias*, *C. praesignis*, *C. timorensis* and *C. aethiopica* comprise 20 of the available species names, with *C. powelli* the only one described as new. Our results contrast with the usual tendency in this family towards the discovery of new species (e.g. Puillandre *et al.*, 2017; Abdelkrim *et al.*, 2018b). All the synonymized species names in this group were established before the 'molecular era of taxonomy', reinforcing the recommendation, which is not always followed (Bouchet & Strong, 2010), of systematically relying on molecular analysis, combined with other data, to delimit species. However, our study also shows that using only molecular delimitation of species while ignoring some key specimens, such as types, would limit knowledge of intraspecific morphological variability, thus also obscuring the ability to relate such variability to extrinsic parameters, such as geographical and bathymetric ranges. In this study, morphological study and taxonomic expertise on types resulted in the extension of intraspecific variability (Fig. 1; e.g. *C. aethiopica* types). This might be explained because, when describing a new species, there can be a strong subjective effect on the choice of the type specimens (usually the largest of a lot). The recent and promising success in sequencing DNA obtained from empty shells (Villanea *et al.*, 2016; Sarkissian *et al.*, 2017) should assist in attributing names to molecularly defined species by sequencing type specimens. However, sequencing shells implies destructive sampling and will therefore possibly not be accepted by many museum curators. Furthermore, identifying and attributing material to species within a species complex still requires considerable taxonomic investigation.

By exploring the intraspecific variability of the shell, in isolation or in relationship to interspecific variability, geographical and bathymetric ranges or ecological data, we emphasize a few remarks that may provide directions for the future study of this group.

GEOGRAPHICAL INTRASPECIFIC VARIABILITY

In *C. aethiopica*, for which many species were synonymized, there are significant geographical variations in the spire whorls. Specimens from the western Indian Ocean were found to have smooth spire whorls, whereas specimens from the central Indo-Pacific were found with either two or three well-marked gemmate cords. Considering the few available discrete shell features, these distinguishable characteristics were used by authors to justify the creation of several species names. No such intraspecific variation in shell sculpture was found in the other species of *Cryptogemma*, although other

geographically structured morphological variability has been observed in the Turridae genus *Lophiotoma* (Puillandre *et al.*, 2017), with shell colour varying from one side of the Indo-Pacific to the other.

ECOLOGICAL VARIABILITY

It has been shown (e.g. Bierne *et al.*, 2003; Hauquier *et al.*, 2017) that some benthic species have clear preferences with regard to the substrate on which they thrive (e.g. sandy/muddy vs. rocky bottom). However, other species are generalists with respect to the substrate. This also seems to be the case for the *Cryptogemma* species. All species were found on both hard and soft substrates, with or without organic matter (e.g. leaves or sunken wood). A remarkable case is *C. tessellata*, for which the three available trawl images showed three different environments (Fig. 12), which were correlated with shell morphology (Fig. 10C, D); specimens found in sandy or spongy environments exhibited a light pale ground colour, whereas the individual found on a volcanic rock bottom had a reddish ground colour. However, the holotype of this species showed an intermediate pattern and was collected 'in mud and sand' (Powell, 1964). More material is needed for a proper study of the potential effects of substrate on shell colour.

SEXUAL DIMORPHISM

Cryptogemma praesignis is the first Turridae species for which apparent sexual dimorphism of the shell has been documented (Kantor & Sysoev, 1991). The (mature) females possess one or several tertiary notches that are probably linked to fertilization according to the authors, because mature males possess an extremely large and muscular penis. The authors proposed the hypothesis that these notches appear periodically during the breeding period, mainly based on the observation of several successive notches on the shells.

BATHYMETRIC ZONATION

Bathymetric segregation between sister species has been shown in molluscan species (e.g. Clague *et al.*, 2012). In the Turridae, it has been found that a pair of sister species, *Lophiotoma abbreviata* (Reeve, 1843) and *Lophiotoma brevicaudata* (Reeve, 1843), show distinct bathymetric preferences, with the former observed at an average depth of 3 m and the latter at an average depth of 15 m (Puillandre *et al.*, 2017). The present study demonstrates that, on a much wider scale, a similar case was found in the *C. praesignis*/*C. phymatias* species pair, with the former species occurring between depths of ~300 and ~1400 m and the latter between ~1400 and ~3000 m (Fig. 5).
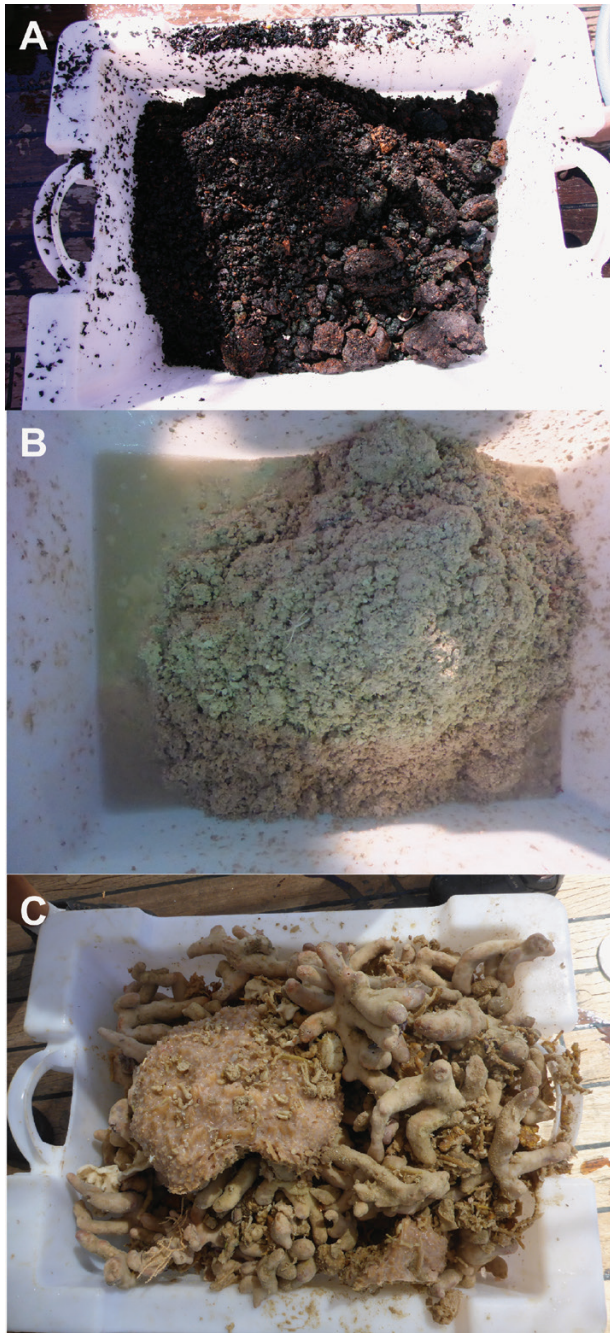
Figure 12. Pictures of trawls from stations where *Cryptogemma tessellata* (Powel, 1964) specimens were found. A, rocky, hard substrate. B, sandy bottom. C, spongy bottom.

This example could be added to the list of models used for studying speciation processes in benthic species with high dispersal capabilities and large geographical distributions, for which a topographic barrier would not provide a satisfactory explanation of genetic isolation (Etter *et al.*, 2005; Zardus *et al.*, 2006).

GEOGRAPHICAL RANGES

Although an Indo-Pacific distribution is common in benthic species, so far no molecularly supported cases of Pacific–Atlantic distribution have been found in benthic gastropods. There are cases of cosmopolitan pelagic gastropods: *Clione limacina* (Phipps, 1774) (Jennings *et al.*, 2010), *Fiona pinnata* (Eschscholtz, 1831) (Trickey *et al.*, 2016) and *Glaucus atlanticus* Forster, 1777 (Churchill *et al.*, 2014). To this extent, *C. phymatias* could be the first documented, molecularly supported case of a benthic gastropod with a Pacific–Atlantic distribution (Fig. 4A). Cases of such molecularly confirmed cosmopolitan benthic species have been found in bivalves (Decker *et al.*, 2012; Laakkonen *et al.*, 2015) and in other phyla, such as Annelida (Meyer *et al.*, 2008; Sun *et al.*, 2016; Tomioka *et al.*, 2016), Arthropoda (Casanova *et al.*, 1998; Havermans *et al.*, 2013) and Algae (Macaya & Zuccarello, 2010). However, human-mediated introduction was strongly suggested for some of these cases, e.g. annelids. Nothing is known of the biological features of *C. phymatias* that would enable such a wide dispersal of larvae.

PROTOCONCH VARIABILITY

As reported by Bouchet & Warén (1979, 1994), many larval shells of deep-water gastropods indicate a planktotrophic larval development, which is generally associated with good dispersal abilities and gene flow. The *Cryptogemma* species are no exception to this, with the protoconch varying from four to 5.25 whorls. However, no correlation was found between the number of whorls of the protoconch in a specimen and its associated depth, implying that, from a certain threshold (e.g. four), the number of whorls is not the only factor determining the ability to disperse. Furthermore, in another neogastropod species complex for which there is a comparable number of protoconch whorls (e.g. Sanders *et al.*, 2017), there is a strict ocean-delimited (e.g. Indian only, Pacific only) distribution. As for *C. phymatias*, the (eroded) protoconch of the holotype of *Bathybermudia carynae* is, to our knowledge, the only one preserved (but slightly eroded) in this species, and it shows no major difference (diameter/height/number of whorls) from other *Cryptogemma* species with regard to this character that could explain its large Pacific–Atlantic distribution.

MORPHOLOGICAL STASIS IN TELEOCONCH

Cryptogemma praesignis and *C. timorensis*, previously assigned to *Ptychosyrinx* by Puillandre *et al.* (2012), show considerable similarity in shell sculpture despite

not being sister species, and the two taxa would be difficult to distinguish without their significant difference in size. These two species represent a clear case of morphological homogeneity in Conoidea, for which other examples have been reported (Kantor *et al.*, 2018). Large-scale morphometrics correlated with phylogeny might provide better characterization and understanding of the conserved '*Gemmula*-like' form across geological time. Some specimens from the Mio-Pliocene have been attributed to species of *Cryptogemma* (see 'Taxonomy'), but an incommensurable number of '*Ptychosyrinx*-like' or '*Gemmula*-like' Turridae from the Palaeogene will probably remain unattributed to a clade until a more comprehensive understanding, characterization and formalization of the family is achieved.

RADULAR MORPHOLOGY

The radula is an important morphological character in conoidean taxonomy. In Turridae, the radula is seemingly similar between congeneric species with few exceptions, such as for *Iotyrris* (Abdelkrim *et al.*, 2018b). *Cryptogemma* is presently one of few genera of Turridae for which the radula has been examined for every representative species. The morphology of the marginal duplex teeth is rather similar among all species, except for slight variation in the development of the accessory limb; either shorter or nearly the same in length as the major limb (*C. timorensis*), or much narrower or nearly of the same width as the major limb (*C. tesselata*). However, we note this with the caveat that the shape of the duplex teeth as inferred from scanning electron microscope images may differ considerably owing to the position of the tooth, thus rendering comparison of different specimens and species imperfect. Additionally, there are large variations between species in the morphology of the central formation in terms of the shape of the central cusp and the degree of development and shape of the lateral flaps, in some cases with distinct elevated edges (*C. tesselata*) and in others with the flaps being barely distinguishable (*C. phymatias*). Another potentially important character is the relative length of the radula, which may differ greatly between species that are otherwise morphologically close (e.g. *C. praesignis* and *C. timorensis*), number of transverse rows of teeth (in *Cryptogemma* varying from 45 to 99) and the relative length of the marginal teeth (from 1.22% of AL in *C. powelli* to 1.9% in *C. praesignis*). Unfortunately, little has been published on relative tooth size in different Turridae lineages and other groups of Conoidea to date.

The above-mentioned characteristics of *Cryptogemma* species have been revealed by morphological and molecular delimitation of species, a practice strongly advised for future studies on Turridae. In particular, it is shown here that morphological differences associated with geographical or ecological diversity within the distributional range of a species may lead to erroneous taxonomic conclusions. Unexpectedly wide geographical distributions, in particular, such as those documented herein, add to the challenges of conoidean taxonomy, notably where morphologically heterogeneous taxa are concerned. This is because material potentially seen as too widely separated geographically to be considered relevant (or where geographically well-separated taxa have not even been considered) may in fact represent conspecific material, a notion supported by the numerous synonymizations herein. Combined with the fact that sampling of the deep sea is infrequent and geographically severely incomplete (potentially masking the presence of morphological clines, which results in the over-emphasis on few, morphologically discrete forms), future studies on deep-sea Conoidea must take such wide distributions into account when embarking upon taxonomic investigation.

Finally, the study of shell variability may serve to produce hypotheses regarding the evolutionary processes that lead to such observed diversity. Indeed, the fact that the molecular-based *Cryptogemma* species were previously split by antemolecular taxonomists into several species each has led us to a re-evaluation and re-interpretation of the intraspecific morphological diversity that we could have neglected otherwise. In this regard, the words of Darwin (1857), 'It is good to have hair-splitters & lumpers', make sense: the splitter reminds lumpers that intraspecific variability should not be ignored, and the lumper reminds splitters that intraspecific variability should not be overinterpreted.

ACKNOWLEDGEMENTS

REFERENCES

Abdelkrim J, **Aznar-Cormano L**, **Buge B**, **Fedosov A**, **Kantor Y**, **Zaharias P**, **Puillandre N. 2018a.** Delimiting species of marine gastropods (Turridae, Conoidea) using RAD sequencing in an integrative taxonomy framework. *Molecular Ecology* **27:** 4591–4611.

Abdelkrim J, **Aznar-Cormano L**, **Fedosov AE**, **Kantor YI**, **Lozouet P**, **Phuong MA**, **Zaharias P**, **Puillandre N. 2018b.** Exon-capture-based phylogeny and diversification of the venomous gastropods (Neogastropoda, Conoidea). *Molecular Biology and Evolution* **35:** 2355–2374.

Barnard KH. 1958. Contributions to the knowledge of South African marine Mollusca. Part 1. Gastropoda; Prosobranchiata: Toxoglossa. *Annals of the South African Museum* **44:** 73–163.

Bickford D, **Lohman DJ**, **Sodhi NS**, **Ng PKL**, **Meier R**, **Winker K**, **Ingram KK**, **Das I. 2007.** Cryptic species as a window on diversity and conservation. *Trends in Ecology & Evolution* **22:** 148–155.

Bierne N, **Bonhomme F**, **David P. 2003.** Habitat preference and the marine-speciation paradox. *Proceedings of the Royal Society B: Biological Sciences* **270:** 1399–1406.

Bonhomme V, **Picq S**, **Gaucherel C**, **Claude J. 2014.** Momocs: outline analysis using R. *Journal of Statistical Software* **56:** 1–24.

Bouchet P, **Kantor YI. 2004.** New Caledonia: the major centre of biodiversity for volutomitrid molluscs (Mollusca: Neogastropoda: Volutomitridae). *Systematics and Biodiversity* **1:** 467–502.

Bouchet P, **Kantor YI**, **Sysoev A**, **Puillandre N. 2011.** A new operational classification of the Conoidea (Gastropoda). *Journal of Molluscan Studies* **77:** 273–308.

Bouchet P, **Strong E. 2010.** Historical name-bearing types in marine molluscs: an impediment to biodiversity studies? In: Polaszek A, ed. *Systema naturae 250 – the Linnaean ark*. Boca Raton: CRC Press, 63–74.

Bouchet P, **Warén A. 1979.** Planktotrophic larval development in deep-water gastropods. *Sarsia* **64:** 37–40.

Bouchet P, **Warén A. 1994.** Ontogenetic migration and dispersal of deep-sea gastropod larvae. In: Young CM, Eckelbarger KJ, eds. *Reproduction, larval biology, and recruitment of the deep-sea benthos*. New York: Columbia University Press, 98–118.

Bouckaert R, **Vaughan TG**, **Barido-Sottani J**, **Duchêne S**, **Fourment M**, **Gavryushkina A**, **Heled J**, **Jones G**, **Kühnert D**, **Maio ND**, **Matschiner M**, **Mendes FK**, **Müller NF**, **Ogilvie HA**, **du Plessis L**, **Popinga A**, **Rambaut A**, **Rasmussen D**, **Siveroni I**, **Suchard MA**, **Wu CH**, **Xie D**, **Zhang C**, **Stadler T**, **Drummond AJ. 2019.** BEAST 2.5: an advanced software platform for Bayesian evolutionary analysis. *PLoS Computational Biology* **15:** e1006650.

Casanova JP, **De Jong L**, **Faure E. 1998.** Interrelationships of the two families constituting the Lophogastrida (Crustacea: Mysidacea) inferred from morphological and molecular data. *Marine Biology* **132:** 59–65.

Chan KO, **Grismer LL**, **Brown RM. 2018.** Comprehensive multi-locus phylogeny of Old World tree frogs (Anura:

Rhacophoridae) reveals taxonomic uncertainties and potential cases of over- and underestimation of species diversity. *Molecular Phylogenetics and Evolution* **127:** 1010–1019.

Churchill CKC, **Valdés Á**, **Foighil DÓ. 2014.** Molecular and morphological systematics of neustonic nudibranchs (Mollusca: Gastropoda: Glaucidae: *Glaucus*), with descriptions of three new cryptic species. *Invertebrate Systematics* **28:** 174–195.

Clague GE, **Jones WJ**, **Paduan JB**, **Clague DA**, **Vrijenhoek RC. 2012.** Phylogeography of *Acesta* clams from submarine seamounts and escarpments along the western margin of North America. *Marine Ecology* **33:** 75–87.

Dall WH. 1918. Notes on the nomenclature of the mollusks of the family Turritidae. *Proceedings of the United States National Museum* **54:** 313–333.

Darwin C. 1857. Letter to J. D. Hooker, August 1st 1875. Darwin Correspondence Project, letter no. DCP-LETT-2130. Available at: http://www.darwinproject.ac.uk/DCP-LETT-2130

Dayrat B. 2005. Towards integrative taxonomy. *Biological Journal of the Linnean Society* **85:** 407–417.

Dayrat B, **Tillier A**, **Lecointre G**, **Tillier S. 2001.** New clades of euthyneuran gastropods (Mollusca) from 28S rRNA sequences. *Molecular Phylogenetics and Evolution* **19:** 225–235.

Decker C, **Olu K**, **Cunha RL**, **Arnaud-Haond S. 2012.** Phylogeny and diversification patterns among vesicomyid bivalves. *PLoS ONE* **7:** e33359.

Dejaco T, **Gassner M**, **Arthofer W**, **Schlick-Steiner BC**, **Steiner FM. 2016.** Taxonomist's nightmare … evolutionist's delight: an integrative approach resolves species limits in jumping bristletails despite widespread hybridization and parthenogenesis. *Systematic Biology* **65:** 947–974.

Edgar RC. 2004. MUSCLE: multiple sequence alignment with high accuracy and high throughput. *Nucleic Acids Research* **32:** 1792–1797.

Etter R, **Rex MA**, **Chase MR**, **Quattro JM. 2005.** Population differentiation decreases with depth in deep-sea bivalves. *Evolution* **59:** 1479–1491.

Fedosov AE, **Puillandre N**, **Achaz G. 2019.** Revisiting use of DNA characters in taxonomy with MolD-a tree independent algorithm to retrieve diagnostic nucleotide characters from monolocus datasets. *bioRxiv* 838151. Available at: https://doi.org/10.1101/838151

Fišer C, **Robinson CT**, **Malard F. 2018.** Cryptic species as a window into the paradigm shift of the species concept. *Molecular Ecology* **27:** 613–635.

Folmer O, **Black M**, **Hoeh W**, **Lutz R**, **Vrijenhoek R. 1994.** DNA primers for amplification of mitochondrial cytochrome *c* oxidase subunit I from diverse metazoan invertebrates. *Molecular Marine Biology and Biotechnology* **3:** 294–299.

Galindo LA, **Puillandre N**, **Strong EE**, **Bouchet P. 2014.** Using microwaves to prepare gastropods for DNA barcoding. *Molecular Ecology Resources* **14:** 700–705.

Giardina CR, **Kuhl FP. 1977.** Accuracy of curve approximation by harmonically related vectors with elliptical loci. *Computer Graphics and Image Processing* **6:** 277–285.

Hasegawa K. 2009. Upper bathyal gastropods of the Pacific coast of northern Honshu, Japan, chiefly collected by R/V *Wakataka-maru*. *National Museum of Nature and Science Monographs*, Tokyo **39:** 225–383.

Hauquier F, **Leliaert F**, **Rigaux A**, **Derycke S**, **Vanreusel A. 2017.** Distinct genetic differentiation and species diversification within two marine nematodes with different habitat preference in Antarctic sediments. *BMC Evolutionary Biology* **17:** 120.

Havermans C, **Sonet G**, **d'Acoz CU**, **Nagy ZT**, **Martin P**, **Brix S**, **Riehl T**, **Agrawal S**, **Held C. 2013.** Genetic and morphological divergences in the cosmopolitan deep-sea amphipod *Eurythenes gryllus* reveal a diverse abyss and a bipolar species. *PLoS ONE* **8:** e74218.

Iglésias SP, **Toulhoat L**, **Sellos DY. 2010.** Taxonomic confusion and market mislabelling of threatened skates: important consequences for their conservation status. *Aquatic Conservation: Marine and Freshwater Ecosystems* **20:** 319–333.

Jennings RM, **Bucklin A**, **Ossenbrügger H**, **Hopcroft RR. 2010.** Species diversity of planktonic gastropods (Pteropoda and Heteropoda) from six ocean regions based on DNA barcode analysis. *Deep Sea Research Part II: Topical Studies in Oceanography* **57:** 2199–2210.

Jovelin R, **Justine JL. 2001.** Phylogenetic relationships within the polyopisthocotylean monogeneans (Platyhelminthes) inferred from partial 28S rDNA sequences. *International Journal for Parasitology* **31:** 393–401.

Kabat AR. 1996. Molluscan types of the Albatross expeditions to the Eastern Pacific described by WH Dall (1908). *Bulletin of the Museum of Comparative Zoology* **155:** 1–31.

Kalyaanamoorthy S, **Minh BQ**, **Wong TKF**, **von Haeseler A**, **Jermiin LS. 2017.** ModelFinder: fast model selection for accurate phylogenetic estimates. *Nature Methods* **14:** 587–589.

Kantor YI, **Fedosov AE**, **Puillandre N. 2018.** New and unusual deep-water Conoidea revised with shell, radula and DNA characters. *Ruthenica* **28:** 47–82.

Kantor YI, **Puillandre N. 2012.** Evolution of the radular apparatus in Conoidea (Gastropoda: Neogastropoda) as inferred from a molecular phylogeny. *Malacologia* **55:** 55–90.

Kantor YI, **Sysoev AV. 1991.** Sexual dimorphism in the apertural notch of a new species of *Gemmula* (Gastropoda: Turridae). *Journal of Molluscan Studies* **57:** 205–209.

Kapli P, **Lutteropp S**, **Zhang J**, **Kobert K**, **Pavlidis P**, **Stamatakis A**, **Flouri T. 2017.** Multi-rate Poisson tree processes for single-locus species delimitation under maximum likelihood and Markov chain Monte Carlo. *Bioinformatics* **33:** 1630–1638.

Kumar S, **Stecher G**, **Li M**, **Knyaz C**, **Tamura K. 2018.** MEGA X: molecular evolutionary genetics analysis across computing platforms. *Molecular Biology and Evolution* **35:** 1547–1549.

Laakkonen HM, **Strelkov P**, **Väinölä R. 2015.** Molecular lineage diversity and inter-oceanic biogeographical history in *Hiatella* (Mollusca, Bivalvia). *Zoologica Scripta* **44:** 383–402.

Lefébure T, **Douady CJ**, **Gouy M**, **Gibert J. 2006.** Relationship between morphological taxonomy and

molecular divergence within Crustacea: proposal of a molecular threshold to help species delimitation. *Molecular Phylogenetics and Evolution* **40:** 435–447.

Macaya EC, **Zuccarello GC. 2010.** DNA barcoding and genetic divergence in the giant kelp *Macrocystis* (Laminariales). *Journal of Phycology* **46:** 736–742.

Martin K. 1935. Oligocaene gastropoden von Buton. *Leidsche Geologische Mededelingen* **7:** 111–118.

Meyer A, **Bleidorn C**, **Rouse GW**, **Hausen H. 2008.** Morphological and molecular data suggest a cosmopolitan distribution of the polychaete *Proscoloplos cygnochaetus* Day, 1954 (Annelida, Orbiniidae). *Marine Biology* **153:** 879–889.

Nguyen LT, **Schmidt HA**, **von Haeseler A**, **Minh BQ. 2015.** IQ-TREE: a fast and effective stochastic algorithm for estimating maximum-likelihood phylogenies. *Molecular Biology and Evolution* **32:** 268–274.

Pante E, **Schoelinck C**, **Puillandre N. 2015.** From integrative taxonomy to species description: one step beyond. *Systematic Biology* **64:** 152–160.

Powell AWB. 1964. The family Turridae in the Indo-Pacific. Part 1. The subfamily Turrinae. *Indo-Pacific Mollusca* **1:** 227–346.

Powell AWB. 1967. The family Turridae in the Indo-Pacific, Part 1a. The Turrinae concluded. *Indo-Pacific Mollusca* **1:** 409–444.

Puillandre N, **Cruaud C**, **Kantor YI. 2010.** Cryptic species in *Gemmuloborsonia* (Gastropoda: Conoidea). *Journal of Molluscan Studies* **76:** 11–23.

Puillandre N, **Fedosov AE**, **Zaharias P**, **Aznar-Cormano L**, **Kantor YI. 2017.** A quest for the lost types of *Lophiotoma* (Gastropoda: Conoidea: Turridae): integrative taxonomy in a nomenclatural mess. *Zoological Journal of the Linnean Society* **181:** 243–271.

Puillandre N, **Kantor YI**, **Sysoev A**, **Couloux A**, **Meyer C**, **Rawlings T**, **Todd JA**, **Bouchet P. 2011.** The dragon tamed? A molecular phylogeny of the Conoidea (Gastropoda). *Journal of Molluscan Studies* **77:** 259–272.

Puillandre N, **Modica MV**, **Zhang Y**, **Sirovich L**, **Boisselier MC**, **Cruaud C**, **Holford M**, **Samadi S. 2012.** Large-scale species delimitation method for hyperdiverse groups. *Molecular Ecology* **21:** 2671–2691.

Robba E, **Sartono S**, **Violanti D**, **Erba E. 1989.** Early Pleistocene gastropods from Timor. *Memorie degli Istituti di Geologia e Mineralogia dell'Università di Padova* **41:** 61–113.

Ronquist F, **Huelsenbeck JP. 2003.** MrBayes 3: Bayesian phylogenetic inference under mixed models. *Bioinformatics* **19:** 1572–1574.

Sanders MT, **Merle D**, **Bouchet P**, **Castelin M**, **Beu AG**, **Samadi S**, **Puillandre N. 2017.** One for each ocean: revision of the *Bursa granularis* species complex (Gastropoda: Tonnoidea: Bursidae). *Journal of Molluscan Studies* **83:** 384–398.

Sarkissian CD, **Pichereau V**, **Dupont C**, **Ilsøe PC**, **Perrigault M**, **Butler P**, **Chauvaud L**, **Eiríksson J**, **Scourse J**, **Paillard C**, **Orlando L. 2017.** Ancient DNA analysis identifies marine mollusc shells as new metagenomic archives of the past. *Molecular Ecology Resources* **17:** 835–853.

Simon C, **Franke A**, **Martin A. 1991.** The polymerase chain reaction: DNA extraction and amplification. In: Hewitt GM, Johnston AWB, Young JPW, eds. *NATO ASI Series. Molecular techniques in taxonomy*. Berlin, Heidelberg: Springer, 329–355.

Sun Y, **Wong E**, **Tovar-Hernández MA**, **Williamson JE**, **Kupriyanova EK. 2016.** Is *Hydroides brachyacantha* (Serpulidae : Annelida) a widespread species? *Invertebrate Systematics* **30:** 41–59.

Sysoev AV. 1996. Deep-sea conoidean gastropods collected by the John Murray Expedition, 1933–34. *Bulletin of the Natural History Museum: Zoology series* **62:** 1–30.

Tesch P. 1915. Jungtertiäre und Quartäre Mollusken von Timor. *Paläontologie v. Timor*: Stuttgart **V:** 1–70.

Thiele J. 1929. *Handbuch der systematischen Weichtierkunde*. Jena: G. Fischer.

Todd JA, **Rawlings TA. 2014.** A review of the *Polystira* clade—the Neotropic's largest marine gastropod radiation (Neogastropoda: Conoidea: Turridae *sensu stricto*). *Zootaxa* **3884:** 445–491.

Tomioka S, **Kondoh T**, **Sato-Okoshi W**, **Ito K**, **Kakui K**, **Kajihara H. 2016.** Cosmopolitan or cryptic species? A case study of *Capitella teleta* (Annelida: Capitellidae). *Zoological Science* **33:** 545–554.

Trickey JS, **Thiel M**, **Waters JM. 2016.** Transoceanic dispersal and cryptic diversity in a cosmopolitan rafting nudibranch. *Invertebrate Systematics* **30:** 290–301.

Tucker JK. 2004. Catalog of recent and fossil turrids (Mollusca: Gastropoda). *Zootaxa* **682:** 1–1295.

Villanea FA, **Parent CE**, **Kemp BM. 2016.** Reviving Galápagos snails: ancient DNA extraction and amplification from shells of probably extinct endemic land snails. *Journal of Molluscan Studies* **82:** 449–456.

Will KW, **Mishler BD**, **Wheeler QD. 2005.** The perils of DNA barcoding and the need for integrative taxonomy. *Systematic Biology* **54:** 844–851.

Zardus JD, **Etter RJ**, **Chase MR**, **Rex MA**, **Boyle EE. 2006.** Bathymetric and geographic population structure in the pan-Atlantic deep-sea bivalve *Deminucula atacellana* (Schenck, 1939). *Molecular Ecology* **15:** 639–651.

SUPPORTING INFORMATION

Additional Supporting Information may be found in the online version of this article at the publisher's web-site.

Appendix S1. *COI* alignment.
Appendix S2. Concatenated (*COI*, 12S and 28S) alignment.

Figure S1. Result of the leave-one-out cross-validation procedure that was used to find the number of principal component axes leading to the best percentage of species predictions.

Figure S2. Results of the ABGD, mPTP and GMYC analysis.

Figure S3. Results of the morphometric analysis without taking size into account.

Table S1. Material examined in this study.